University of Verona

Department of Neuroscience, Biomedicine and Movement Sciences

Graduate school of Life and Health Sciences

Doctoral program in in Neuroscience, Psychology and Psychiatry

Cycle XXIX

Neural correlates of visual perceptual awareness and short-term memory

S.S.D. M-PSI/01

Coordinator: Prof. Leonardo Chelazzi

Supervisor: Prof. Carlo Alberto Marzi

Ph.D. student: Alice Bollini

✓ Licenza Creative Commons per preservare il Diritto d'Autore sull'opera.
(consigliata)

✓ *Neural correlates of visual perceptual awareness and short-term memory*

Alice Bollini

Tesi di Dottorato

Verona, 20/02/2017
ISBN

"Philosophy [nature] is written in that great book which ever is before our eyes -- I mean the universe -- but we cannot understand it if we do not first learn the language and grasp the symbols in which it is written. The book is written in mathematical language, and the symbols are triangles, circles and other geometrical figures, without whose help it is impossible to comprehend a single word of it; without which one wanders in vain through a dark labyrinth."

Galileo Galilei

INDEX:

1. Introduction
2. Methods
3. Results
4. Discussion

- **Chapter4: Does Cognitive Training Enhance Intrinsic Brain Connectivity? A MEG study**

1. Introduction
2. Methods
3. Results
4. Discussion
5. Future Direction

- **References**

- **Acknowledgments**

- **Abstract**

The general aim of the experiments described in my Thesis is to study how the brain creates a representation of the external world. In particular I have investigated three different aspects that make possible our subjective visual experience: Visual processing, short-term memory and the resulting perceptual awareness.

The first part of the Thesis deals with visual perception and visual awareness by describing experiments involving behavioral tasks in brain damaged and healthy subjects. In particular, it is focused on when and where awareness arises. We used moving stimuli, because they can reach the motion area V5 bypassing the primary visual area V1 and therefore motion represents a suitable feature to study unconscious vision. Chapter 1 deals with the differences in the event-related potential (ERP) response between static and moving gratings in healthy subjects. We found that motion selectively affects N1, i.e. a negative component mainly recorded in the posterior electrodes of the right hemisphere. This study was preparatory to the experiment described in Chapter 2 in which we tested patients with hemianopia to understand how plastic reorganization of visual areas can reinstate unconscious ("blindsight") or conscious vision. As to the main result of this study, we found one patient who showed both implicit above chance discrimination performance with motion stimuli and an unrelated presence of degraded awareness of the stimulus presented to the damaged field. As to ERP recording, we found reliable responses correlating either with the patient's unconscious above chance behavior (Late Posterior Negativity) or with the subjective experience of degraded vision during stimulus presentation (N1-P2a components). Taken together, these results suggest an onset of visual awareness (albeit rudimentary) during early visual processing.

The second part of the Thesis deals with short-term memory (STM), that is, a crucial processing stage for the representation of the external world. The aim of this part is to investigate inter-individual differences in STM capacity and the effect of cognitive training. Instead of using a classical approach in which subjects are actively involved

in a task we employed a resting state paradigm. Chapter 3 describes a study using magnetoencephalography (MEG) to investigate connectivity at rest to assess if individual differences in intrinsic brain activity can predict inter-subject variability in STM. We found that intrinsic brain activity can predict the behavioral performance tested outside the scanner, and that can play a key role in performing a successful STM task. In Chapter 4 we have tested the possibility that an intensive STM training could modify the functional connectivity, that is, if there are differences in resting state networks (RSNs) before and after STM training. In particular, we asked whether three different kinds of training (Verbal, Visual and Spatial STM) could affect connectivity in the fronto-parietal RSNs and interconnected areas. We found that, at behavioral level, training had a specific effect on the different kinds of task, while at connectivity level, we did not find any changes in the RSNs. Presumably, the absence of a significant effect might be due to the use of three different types of training that increased the results variability. In addition, probably the training was too short to have effects on intrinsic brain activity, even though it was sufficient to improve behavioral performance.

- **General Introduction**

Seeing the words in this page, or a wooden desk, or a landscape outside the window seems to be an easy process. But it is not. It requires a cascade of many neuronal events, which must be encoded into brain activity in fractions of seconds. The main goal of this thesis is to study the neurophysiological correlates of the brain processes that enable such an internal representation of the external world.

The idea that all aspects of cognition can be expressed solely in term of neurons and cortical circuitry is well expressed in the book *The Astonishing Hypothesis* (Crick, 1994) where the author asserts that "a person's mental activities are entirely due to the behaviour of nerve cells, glial cells, and the atoms, ions, and molecules that make them up and influence them". At the basis of consciousness, there is a complicated and unique mixture of different mental states, from being visually aware of an object (visual awareness) to the more complicated recognition of oneself as single human being separated from the rest of the world (self-consciousness). This process or processes are subserved by a neural circuitry consisting of cortical networks that involve many brain areas whose activity correlates somehow with the fact of being conscious of something. Therefore, the best way to explore consciousness in a scientific way is to investigate the neural bases of perceptual awareness. The visual system represents a very important milestone for cognitive neurosciences because its structure and physiology are well known and therefore amenable to experimental investigation. Studying visual awareness offers many advantages with respect to other forms of consciousness. First of all, the human visual system is very similar to that of some primates and this allows experiments that for ethical reasons are not possible in humans. Moreover, human beings base their external world representation mostly on vision by virtue of processes highly structured and rich of information.

In essence, the aim of this thesis is to study the neural correlates of visual experience, from simple perception to the consciousness of what we see and the use of that information to interact with the world. Visual experience is characterized by many

different stages: From transduction of light in the retina at the lowest sensory processing level to complex operations of categorization which require the involvement of higher cognitive-level processing subserved by the cerebral cortex. When we see, for example, a face in the real world the light that contains the visual information is detected by the retina and goes through a sequence of different stages to various visual areas in the brain in a semi-hierarchical way. This process is structured in such a way as to transform unconscious information into perceptual awareness. This means that when we consciously perceive a face the retinal information to become explicit requires the activation of a pattern of neurons, or entire networks whose activity enables conscious perception. This is the topic of this Thesis: how visual information reaches consciousness passing from one visual area to another. It is well known that visual information is processed in many streams, for example, colour, shape, and movement are processed by different brain areas, but eventually the information processed along different streams comes together and proceeds to a stage where it can be used to interact with the external word.

In this thesis, I will investigate three different aspects of visual experience: visual processing, visual awareness, and short-term memory.

The first part will deal with visual perception and visual awareness by describing experiments carried out with a classic approach that involves behavioural tasks in brain damaged and healthy subjects. In particular, it will be focused on when and where the neural correlates of consciousness (NCC) arise, that is, on the temporal aspects of processing of unconscious and conscious visual information. There are two basic experimental approaches to study visual awareness: One is to study healthy participants with visual stimuli rendered invisible or barely visible and comparing the neural response to the same stimuli when yielding conscious versus unconscious performance. The other approach is to find out whether patients, who cannot have access to visual information directly because they lost vision as a result of damage to the visual cortex, are still able to respond, albeit unconsciously, to a visual stimulus. This phenomenon is known as “blindsight” (Weiskrantz et al, 1974). Knowledge of

the timing of shifts from unconscious above-chance visually guided behaviour (blindsight) to partial or total perceptual awareness would be crucial for understanding the neural as well as cognitive underpinnings of consciousness. For this reason, we decided to investigate the timing of NCC by studying the electrophysiological responses to visual stimuli in patients with cortical blindness. In particular, we used moving stimuli which represent a privileged input for these patients because there is evidence that visual motion information can reach cortical areaV5 bypassing V1, the primary visual area. In order to do this, as a preliminary experiment, we recorded the electrophysiological response to moving square-wave gratings in a group of healthy participants. In Chapter 1, we studied the differences in the event-related potential (ERP) response between static and moving gratings. We found that motion affects the N1 component, i.e. a large negative component mainly recorded in the posterior electrodes of the right hemisphere. This study was preparatory to the experiment described in Chapter 2, in which we tested patients with hemianopia as a consequence of cortical lesions in order to understand which kind of lesion (and the resulting plastic reorganization of visual areas) can explain the presence or absence of perceptual awareness, or the presence or absence of blindsight. In particular, in Chapter 2 is described a study designed to cast light on the timing of these phenomena by using EEG, i.e. a technique which can give important information on the timing of NCC. As the main result of this study, we found one patient who showed both above chance performance with motion stimuli and also an unrelated presence of awareness of the stimulus presented to the hemianopic field. Remarkably, in the blind field of a hemianopic patient we found a reliable ERP response in the time window of N1 mostly present in the ipsilesional (left) posterior electrodes. This ERP response was related to the patient's feeling of something appearing in the blind field and was present with both static and motion stimuli. In addition, we found that the above-chance unconscious orientation discrimination was present only for moving stimuli and was witnessed by a late negative component in the contralesional (right) posterior electrodes. This ERP component was present only for motion stimuli and can be considered as the neural correlate of a form of

blindsight enabling feature discrimination only when stimuli are moving and is subserved by the intact hemisphere most likely through an interhemispheric transfer.

The second part of the Thesis deals with short-term memory (STM), that is, the ability to retain a small quantity of information for a short time for further elaboration. STM is fundamental for the representation of the external world, for its consolidation into long-term memory and for the interaction with the environment. Traditionally, STM and awareness are considered strictly related processes. Not all the information of the external world reaches awareness, and STM represents the process that selects which information will be accessible to higher-level cognitive processes and become conscious (Soto and Silvanto, 2014; Sligte, 2008). The aim of this part of the thesis is to investigate inter-individual differences in STM capacity and if this processing stage can be improved by cognitive training. Instead of using a classical approach in which the subject is actively, involved in a task we decided to use a new methodology to examine the brain while the subject is literally told to do nothing, a condition of spontaneous cerebral activity known as resting state. It is known that this activity is spatially and temporally structured in networks, the so-called resting-state networks. This new methodology enabled us to explore if individual differences in intrinsic brain activity can predict inter-subject variability in STM assessment. Chapter 3 describes a study making use of magnetoencephalography (MEG) to investigate brain activity at rest. In this study, we have documented the feasibility of MEG as a tool to explore resting state connectivity. Moreover, we have demonstrated that intrinsic brain activity can predict the behavioural performance tested outside the scanner, and that can play a key role in performing a successful STM task.

Because information in the external world is constantly changing, it becomes crucial to understand how the brain updates these representations. In Chapter 4, we have investigated how intrinsic brain activity changes in response to the environment and in particular if it is possible to modify the intrinsic brain connectivity as a result of cognitive training. This could provide new insight on possible procedures of

cognitive rehabilitation. It is very important to understand not only how brain plasticity operates spontaneously after a lesion but also how an intensive training could help recover a damaged function. To do this we examined if there are any differences in resting state networks before and after STM training. In particular, we investigated how three different kinds of training (Verbal, Visual, and Spatial STM) could affect the connectivity in the fronto-parietal networks or in the areas, which communicate with them. As a result of this study, we found that, at behavioural level, training had a specific domain-effect, that is, the improvement after training was mainly restricted to the specific domain trained. At connectivity level, we were not able to find any changes in the fronto-parietal RSNs. The absence of a significant effect is probably due to the complication of using three different types of training that created a great variability in terms of connectivity. This variability made it difficult that an effect could survive multiple statistical comparisons. On the other hand, it could be that training was too short to create changes in the intrinsic brain activity, even if its timing was enough to improve the behavioural performance.

In conclusion, I believe that taken together these results are useful not only to understand how the brain builds up his own representation of the world, but also for understanding how the brain changes through a plastic cortical reorganization after severe injury.

- **Part I: Neural correlates of visual awareness in healthy participants and hemianopic patients**

Chapter 1
Cerebral correlates of motion perception

1. Introduction

Everything surrounding ourselves is dynamic. This makes motion perception one of the most important processes of the visual system because it guides us in moving in the external world and also provides important clues for other visual functions such as for example pattern discrimination. It has been clearly demonstrated that in the human brain there is a specialized area for motion processing. This area is known as V5/MT+ and has a homologous in the medio-temporal cortex (MT) of non-human primates. It has been demonstrated that V5/MT+ receives input from the striate cortex (V1), and extra-striate cortices (V2 V3 V4 and V6), see Galletti et al., 2001. Importantly, it has been shown that there are four pathways that from the retina reach the motion area directly bypassing V1 (Ffytche et al., 1995; Buchner et al. 1997; Schoenfeld et al., 2002). Studies on monkey found that these pathways involve three different subcortical structures (see figure 1, Tamietto and Morrone, 2016): Lateral Geniculate Nucleus (LGN) (Sincich et al., 2004; Schimd et al.,2010); pulvinar (Berman and Wurtz, 2010) and superior colliculus (SC) (Gross,1991).

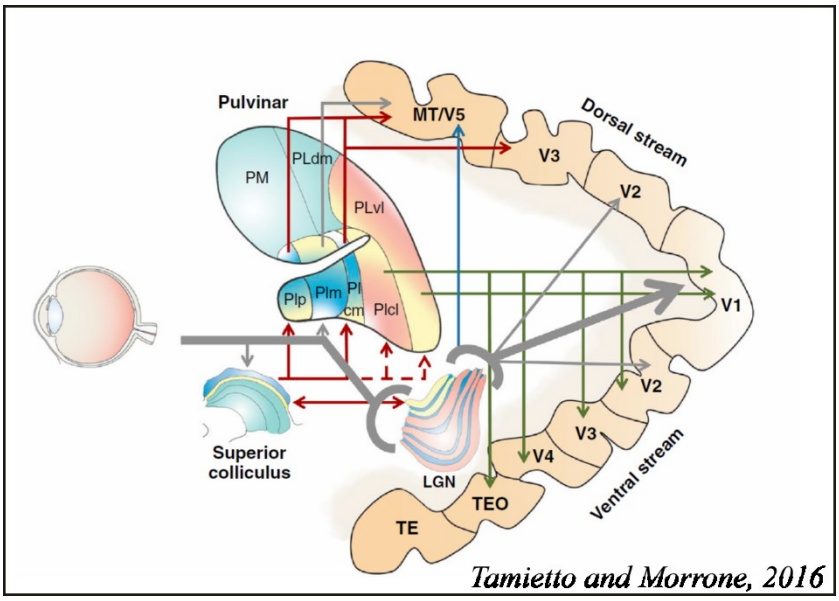

Figure 1. Connections from the eye to the visual cortex involving intermediate relays in LGN, superior colliculus and pulvinar. Gray arrows indicate direct projections from the retina with thicker lines showing the major geniculo-striate pathway involving LGN and targeting V1. Red arrows indicate projections originating from the superior colliculus and reaching the dorsal stream cortical areas via the pulvinar, with dashed lines showing disputed input to subdivisions of the pulvinar. Green arrows indicate projections from pulvinar subnuclei to areas along the cortical ventral stream. The blue arrow indicates projections from the Koniocellular layers of LGN to area MT. In LGN and superior colliculus, yellow layers indicate Magnocellular, blue Koniocellular, and pink Parvocellular channels. In the pulvinar these pathways are not clearly segregated and shaded blue-yellow; pink-yellow colors indicate the conjoint presence of the respective channels in given subdivisions. Light green denotes areas of the superior colliculus and pulvinar not interesting for the present purposes. Abbreviations: PIcl, pulvinar inferior centro-lateral; PIcm, pulvinar inferior centro-medial; PIm, pulvinar inferior medial; PIp, pulvinar inferior -posterior; PLdm, pulvinar lateral dorso-medial; PLvl, pulvinar lateral ventro-lateral; PM, pulvinar medial; TE,temporal inferior rostral; TEO, temporal inferior posterior.

The detailed anatomo-functional study of these pathways can cast light on the residual function of blindsight patients (that is, patients who lost a part of visual field, due to V1 damage but can reliably respond to visual stimuli that they do not consciously see). In particular, EEG studies can help understand which pathway/s can explain the various kinds of blindsight abilities. Some electrophysiological studies found a very early activity of V5/MT+ which bypasses V1 activity (Schmolesky et al., 1998) and a post stimulus-onset latency ranging from 35 ms to 120 ms. Thus, EEG, and, in particular, the study of the evoked response to a motion stimulus (Motion ERPs), can clarify the timing of motion processing. In particular, it is well

known that the motion onset effect is marked in the N1-N2 time domain, with a source localization in V5/MT+ (Lorteije et al., 2009; Pitzalis et al., 2012). However, other studies found an early effect also in P1 time domain (De Vries et al., 1989; Schoenfeld et la., 2002). In order to better understand the Motion ERPs dynamics we designed an experiment where we tested healthy participants while performing an orientation discrimination task with motion and static stimuli. This study was preparatory to that with patients and helps understand how motion is processed in an undamaged brain. This experiment is described as part of a recently submitted paper by Bollini et al. (submitted).

2. Methods

2.1. Participants

Eight healthy participants (3 males, 27±6 years old) were tested as visually intact controls. All were right-handed with normal or corrected-to-normal vision and with no history of neurological or cognitive problems. All signed an informed consent prior to participating in the study and were free to withdraw at any time. The study was approved by the Ethics Committee of the Azienda Ospedaliera Universitaria Integrata of Verona and of the ERC and conducted in accordance with the 2012-13 Declaration of Helsinki.

2.2. Experimental procedure

Participants were tested in a light-dimmed room. They were comfortably seated in front of a 24-inch LCD monitor (ASUS VG248) with a refresh rate of 144 Hz driven by a PC used for stimulus presentation. The stimuli were black and white square-wave gratings of 4o of visual angle with a Michelson contrast of 100 % against a grey background of 18.33 cd/m2 and a spatial frequency of 0,8750 c/°. The gratings mean luminance was 29.46 cd/m2.. They could have either a vertical (0°) or horizontal (90°) orientation and could be static or moving (apparent motion), vertical gratings drifting to the right and horizontal gratings drifting downward. Stimuli were

generated using PsychToolBox-3 (Brainard, 1997) running on Matlab 2013b (MathWorks Inc.). The retinal eccentricity of stimulus presentation used was 9° measured from the inner portion of the display to the central fixation point along the horizontal meridian and 7° along the vertical meridian in the upper visual field.

The behavioural paradigm (Fig.2) consisted of four different trial blocks repeated four times (960 trials) and alternating in the following order: Static gratings in the right and then in the left field, moving gratings in the right and then in the left field. In patients, the sequence started from the intact field. A block consisted of 60 trials of vertical or horizontal gratings presented in random order; in 30% of the trials, no stimuli were presented (catch trials).

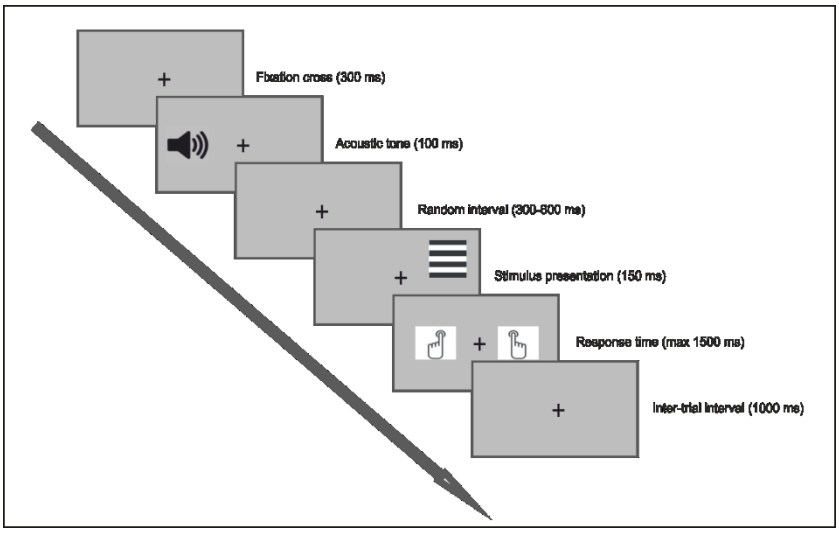

Figure 2. Experimental procedure: First, a fixation cross was presented for 300 ms followed by an acoustic tone lasting 100 ms. After a random interval between 300-600ms the stimulus was presented for 150 ms. The subject had 1500 ms to respond by pressing a button on the keyboard. The inter-trial interval lasted 1000 ms.

Participants were asked to perform an orientation discrimination task regardless of whether the stimuli were moving or static. Trials started when a fixation cross of 0.15° appeared in the centre of the screen for 300 ms, followed by an acoustic tone (1000 Hz). After a random interval (300-600 ms) the stimulus was presented to the left or right upper hemifield for 150 ms and participants had 1500 ms to press as quickly as possible one of two keyboard keys, using the right or the left index finger

to signal a vertical or horizontal grating, respectively (counterbalanced across subjects). The inter-trial interval was 1000 ms. Importantly, patients were asked to press one of the two keys also when they did not perceive any stimulus in the blind hemifield (including catch trials).

2.3. EEG recording and analysis

EEG activity was continuously recorded from 64 active electrodes (actiCap, Brain Products GmbH, Munich Germany) placed according to the 10-10 International System and was acquired in one experimental session with BrainAmp (Brain Products GmbH, Munich, Germany) and BrainVision software. All scalp electrodes were referenced online to the left mastoid and re-referenced offline to the arithmetically derived average of left and right mastoids. The ground electrode was placed at AFz position. Additionally, horizontal and vertical eye movements were recorded with four electrodes placed at the left and right canthi and above and below the right eye, respectively. Impedance was kept below 5 kΩ for each electrode. The EEG was recorded at 1000 Hz sampling rate with a time constant of 10 s as low cut-off and a high cut-off of 1000 Hz with a 50 Hz notch filter. The EEG signal was processed offline using a combination of custom scripts written in Matlab 2013b (MathWorks Inc.) and EEGLAB toolbox (Delorme and Makeig, 2004). Continuous data were bandpass filtered offline between 1 and 100 HZ. The continuous raw data were visually inspected, large signal jumps such as muscle twitches or electrode cable movements were rejected, and bad channels were interpolated. Independent component analysis (ICA) decomposition with logistic infomax algorithm Runica (Makeig et al. 1996; Bell and Sejnowski, 1995) was performed (Lee et al., 1999) to separate brain and non-brain source activities. Stereotyped artefacts like blinks were corrected by identification of the corresponding ICs. After artefact correction and source localization, a mean of 24 ICs (STD=4.83) remained for each subject. Next, data epochs were extracted (from -200 before to 800 ms after stimulus presentation) and baseline corrected (from -200 ms to stimulus onset). At this point, the data were downsampled to 250 Hz. Next, point-by-point non-parametric ANOVAs or T-tests

based on 5000 permutation testing were performed in order to identify differences among catch trials and the motion and static condition. A FDR correction (Bejamini & Yekutieli, 2001) was applied to correct for multiple comparisons. We used non-parametric statistics because they offer many advantages: first of all, they are highly appropriate for correcting multiple comparisons in EEG data, second this kind of statistics do not rely on distribution assumptions, this means that are not a priori assumptions regarding where and when there will be an effect, lastly they account for multiple comparisons and avoid uncontrolled false positive rate.

In addition, ERP envelope (i.e. minimum and maximum of all electrodes at every time point) was used to calculate which three clusters of IC gave the largest source contribution to the EEG signals in term of PVAF (percent of variance accounted):

$$PVAF(IC) = 100-[100*mean\ (var\ (all\_data - back\_proj))/mean\ (var(all\_data)]$$

Where "var" stands for variance; "data" refers to EEG signals, as well as the matrix channels x time-points; finally, "back_proj" refers to the ERP activity of the selected IC back-projected to the scalp ERPs (as a forward projection from cortical source to the scalp channels), thus PVAF indicates the contribution of the IC to the ERP (Lee et al., 2015). In order to calculate the cluster of ICs across subjects we used an automated K-means algorithm procedure on scalp maps, ERPs, and dipole localizations. With this procedure, we selected the clusters of ICs that maximally accounted for variance at the electrodes. We used this procedure to explore the nature of ERP components; in particular, we focus on C1, P1, N1, and P300.

3. Results

3.1. Behaviour

The performance of subjects was accurate and fast: Right static stimuli = 97.3% correct responses and Reaction Time (RT) = 567 ms; right moving stimuli=98.6%, RT = 554ms; left static stimuli = 97.8%, RT = 561 ms; left moving stimuli = 98.7%, RT = 554 ms). This indicates a low task difficulty. There were no statistically

significant differences in accuracy or RT between hemifields and between moving and static stimuli (Fig.3).

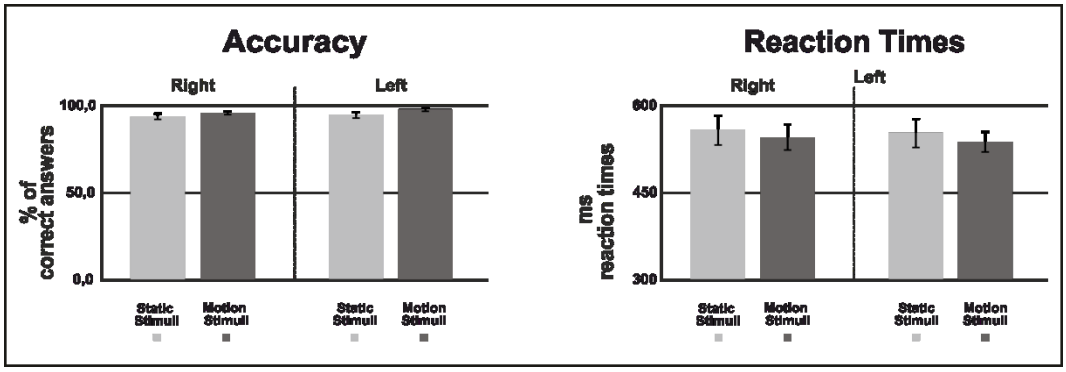

Figure 3. Behavioural results: In the left, panel the mean percentage of correct responses for each experimental condition. In the right side, the mean of response times for each experimental condition.

3.2. EEG

Figure 4 shows the ERP responses as recorded at electrode Pz. With a peak detection procedure we found a negative C1 at 75 ms, the sign being in keeping with the site of stimulus presentation in the superior quadrant of the visual field (Jeffreys and Axford, 1972) and therefore with a V1 generator; moreover, a P1 at 110 ms; a N1 at 185 ms and a large P3 between 310 and 480 ms.

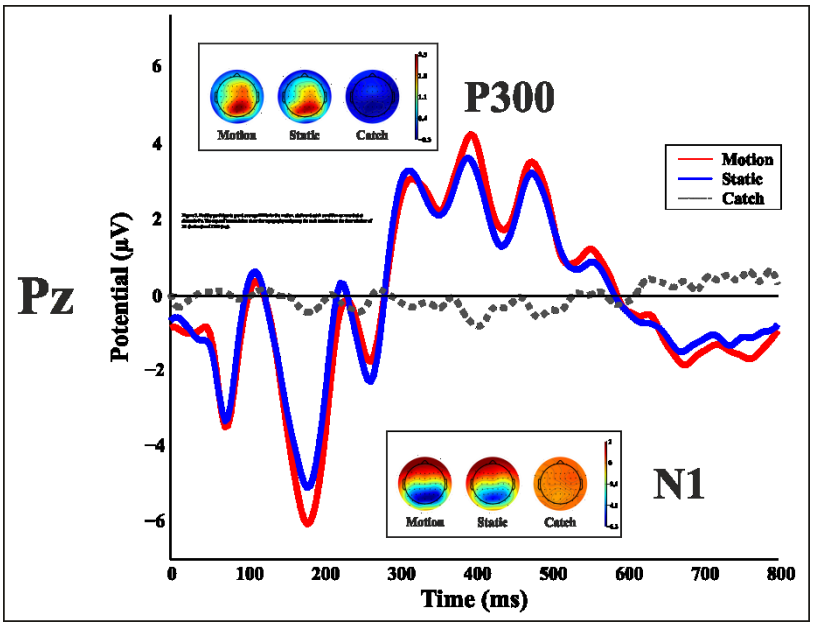

Figure 4. Healthy participants grand average ERPs for the motion, static and catch condition as recorded at electrode Pz. The top and bottom inlets show the topography scalp map for each condition at the time window of N1 (bottom) and P300 (top).

A 5000 permutation ANOVA was conducted for the three conditions of stimulus presentation (static, motion and catch regardless the side of stimulation). The main results are shown in Fig.5: Significant FDR corrected p-values ranged between 0.00084975 and 0.04977. As shown by the raster plot the main differences between the three conditions were in the peaks timing (P1 N1 and P300), in particular in the centro-parietal and posterior channels. In order to assess the differences between static and motion condition we ran non-parametric t-tests for the peak time-window.

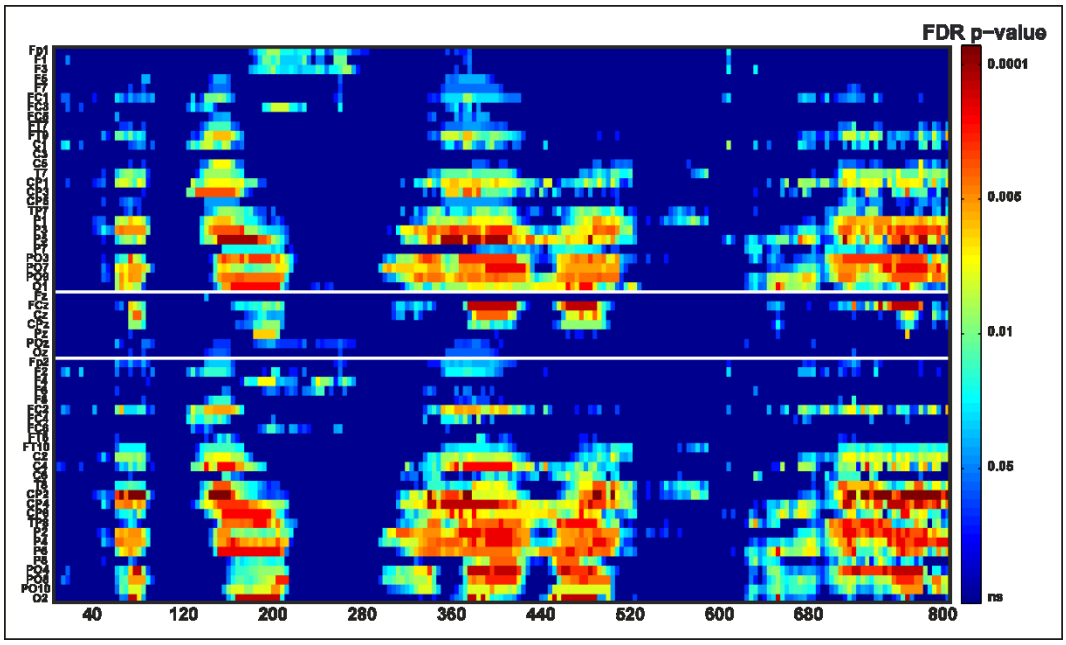

Figure 5. Raster plot resulting from the permutation ANOVA across all electrodes and the three conditions regardless the side of the stimulation. Colour points represent the p values after the FDR correction for multiple comparisons. Ordinates: left, electrode sites; right, p- values. Abscissae: post-stimulus onset time (ms).

The permutation t-test on the mean amplitude of the peaks showed a difference between static and moving stimuli only for the N1 component with a larger negative amplitude at the following electrodes: CP6, P1, P2, P4, P6, P7, P8, PO3, PO4, PO8, PO10, O1, Oz, O2 (with a p-value<0.05), as shown in figure 6. These differences were mainly observed in the right hemisphere regardless of the side of visual field of stimulus presentation.

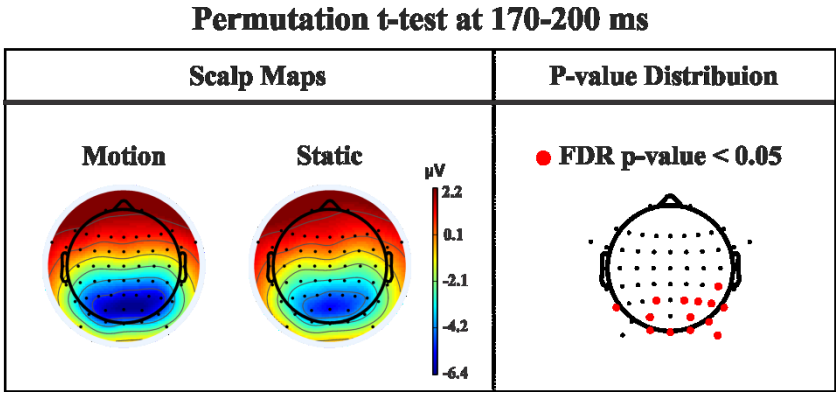

Figure 6. Non-parametric t-test between Motion and Static conditions in N1 time window from 170 ms to 200 ms. On the left side: Scalp maps of the Motion and Static condition; on the right side the electrodes with p-values under 0.05 after the correction for multiple comparison.

To better understand the origin of the above ERP components we calculated the contribution of the three largest clusters of ICs to the grand mean ERPs, computing the mean across the maximum ERP envelope in the time intervals C1, P1, N1 and P300. These intervals were used previously for the t-test analyses. The results of this procedure showed that each ERP component is mainly formed by the posterior component and that the three clusters of ICs explained approximately 70% of the summed PVAF (C1: Static 85.4%, Motion 72.4; P1: Static 68.4%, Motion76.1%; N1: static 63.4%, Motion 63.5%; P300: Static 65.4%, Motion 72.3%). As shown in figure 7, it is interesting to note that the C1 is formed by the same clusters of ICs in both motion and static condition while N1 is partially formed from the same clusters of ICs and one lateralized cluster in the right hemisphere for the motion condition.

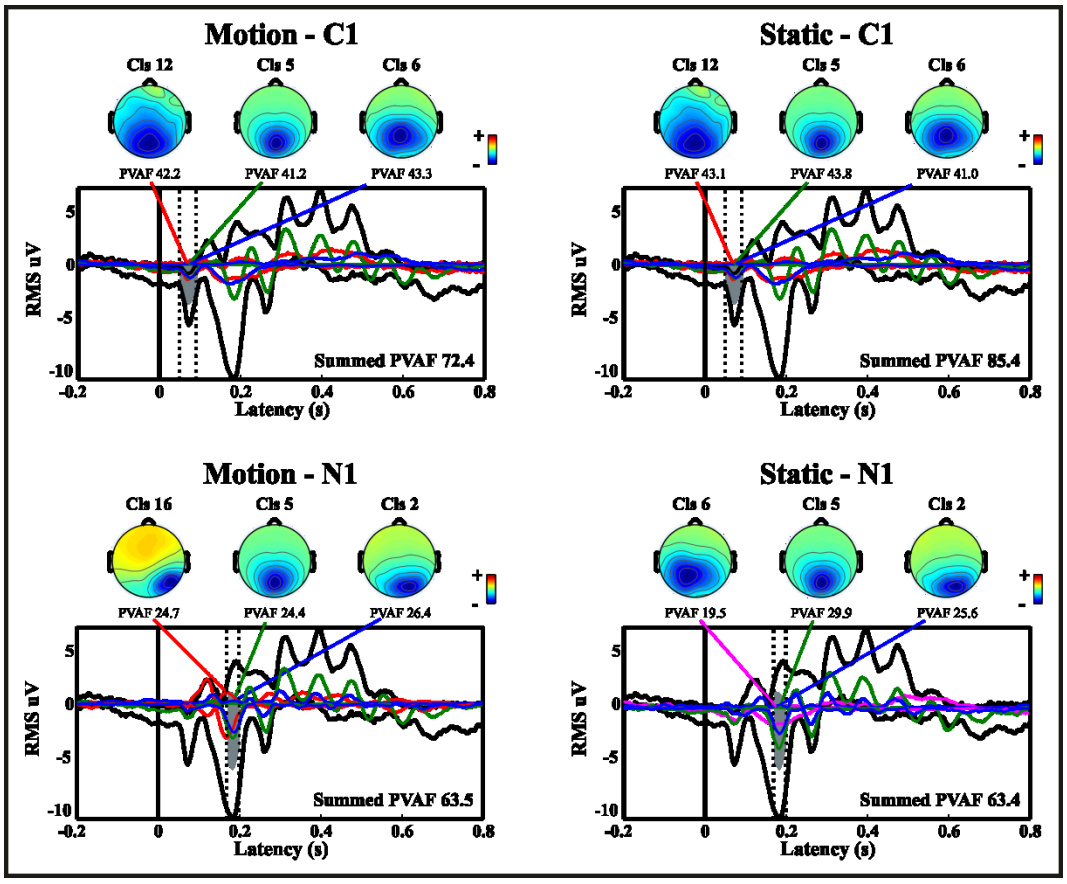

Figure 7. Grand mean of C1 and N1 ERP envelopes plotted separately for both stimulus conditions. The black line in each plot represent the scalp-recorded data envelope, that is, the minimum and maximum potentials at all channels at each latency. The top and bottom of the grey-filled areas give the grand mean activity of the back-projected independent components in the corresponding cluster of ICs. The mean PVAF by the independent components is given. The dotted lines represent the time window considered for the Summed PVAF.

4. Discussion

The aim of this study was to investigate the EEG evoked response to motion stimuli in an undamaged brain. In particular, we were interested to understand the difference between static and drifting stimuli. The results will be compared to the ERP response of hemianopic patients in both blind and sighted hemifield. In this study, we found that this kind of stimulation evokes a typical ERP response with a negative C1, a P1, a N1 and a large P300. In contrast, the catch condition, i.e. the absence of any stimulation, does not evoke any reliable activity. Moreover, we found a significant

difference between the motion and the static condition in the N1 time window consisting in a larger negative amplitude for the motion than the static stimuli. These results are in line with previous studies (Schoenfeld et al., 2002; Lorteije et al., 2009; Pitzalis et al., 2012), a similar N1 effect was found by Coch and colleagues, 2005, in both adults and children using drifting gratings. An important point to highlight is that the effect of the motion stimulation is more prominent in the right hemisphere, as indicated by t-test and envelope analyses (Fig. 6 and 7). This can provide useful information for the study with hemianopic patients because can predict different behaviours and different ERP correlates depending upon the lesion side. Although Chenk and Zihl (1996) studied a large group of patients and concluded that “neither the right nor the left hemisphere possesses a "dominance" for visual motion perception”, a recent study of Kavcic et al. (2015), found an interhemispheric transfer of motion information in hemianopic patients following left but not right hemisphere damage.

Chapter 2
A glimpse of light beyond the darkness: Neural responses from a blind visual hemifield

1. Introduction

We are always interacting with the ever-changing external world. To understand how the brain creates a representation of it implies understanding how information reaches our consciousness. The search for the neural correlates of consciousness (NCC) is undoubtedly one of the most exciting and challenging enterprises of cognitive neuroscience (see Panagiotaropoulos et al., 2014). One approach to investigate NCC is to find out what are the cognitive and neural mechanisms that enable some patients with cortical blindness to perform above chance in various visual tasks despite lack of perceptual awareness. This approach was pioneered by Poeppel et al. (1973) and Weiskrantz et al. (1974) who demonstrated that stimuli presented to the blind hemifield of hemianopic patients could be reliably spatially located either with saccadic or manual pointing movements despite lack of perceptual awareness. Following these initial findings, a vast series of studies has provided precious information on the functions that can be carried out without perceptual awareness, a phenomenon termed "blindsight" by Weiskrantz et al. (1974). This approach has yielded key information for understanding the limits and the capacities of unconscious vision using both behavioural paradigms and neuroimaging techniques (like TMS, EEG or fMRI). One of the main unanswered questions concerns the temporal aspects of the processing of unconscious with respect to conscious visual information. That is, at what processing stage and at what corresponding neural level does perceptual awareness emerge? Certainly, fMRI is not ideally suited for answering this question given its relatively low temporal resolution. In contrast, non-invasive electrophysiological techniques such as electroencephalography (EEG), and in particular ERP, with its optimal temporal resolution constitute an invaluable tool that we have used in the present study. From a theoretical point of view there two main positions on the time of emergence of perceptual awareness: On one side, there are theories positing an early activation of the visual cortex as a crucial site, such as,

for example, the Recurrent Processing (RP) theory of Lamme et al. (2010). On the other side, there are theories positing a later activation in fronto-parietal areas, such as for example the global workspace theory (GWT) proposed by Dehaene and Naccache (2001). Both theories are controversial: For example, it has been shown that some patients with V1 lesion could still report some form of awareness especially with fast-motion stimuli (Barbur et al., 1993; Milner, 1998; ffytche et al., 1996; ffytche and Zeki, 2011) or with TMS stimulation of the intraparietal sulcus (IPS) (Mazzi et al., 2014) and this is not in keeping with the RP theory. By the same token, also the GWT has received some criticism, e.g. as a result of the finding of a negative ERP component recorded around 200 ms post stimulus onset, i.e. in N1 domain, over posterior cortical areas that correlates with different degrees of visual awareness (Koivisto and Grassini, 2016; Tagliabue et al., 2016). To try and further explore the problems raised by the above controversial picture, in the present study we focused on assessing whether and at what latency stimuli presented to the blind hemifield of hemianopic patients can elicit visually evoked responses that might correlate with the presence of blindsight or residual conscious vision. ERP studies of blindsight are rather scanty: There have been some attempts, with contrasting results, to find reliable ERP responses following blind hemifield stimulation, see Kavcic et al. (2015) for a review. In a pioneering paper, Shefrin et al. (1988), found in one hemianopic patient with blindsight a P300 component when a target word was presented to the blind field. However, interestingly, no P100 was found in this as well as in the hemianopics without blindsight tested. In Kavcic et al. (2015) study there was no evidence of reliable behavioural response to moving dots presented to the blind hemifield and no evidence of ERP response in the damaged hemisphere. However, they found that the damaged hemisphere could be activated via interhemispheric transfer from the intact hemisphere. Importantly, this was the case only in left brain-damaged patients suggesting that the right hemisphere has a special ability to transfer visual motion information to the other hemisphere, see behavioural evidence for this possibility in Marzi et al., 1991. At any rate, apart from possible transfer asymmetries, Kavcic et al's results show that the presence of viable callosal

or extracallosal connections between intact and damaged hemisphere is of key importance for understanding the mechanisms of plastic reorganization possibly leading to partial or total restoration of vision (see discussion in Celeghin et al., 2015b).

In the present study, we tested five hemianopic patients with different brain lesions in an orientation discrimination of moving or static visual gratings while recording ERPs. Because the main goal of this work was to evaluate how the plastic neural reorganization due to different lesions can induce different kinds of behaviour, we analysed our patients as single-cases. The description of this study is partially contained in Bollini et al. (submitted).

2. Methods

2.1. Participants

All the patients signed an informed consent prior to participating in the study and were free to withdraw at any time. The study was approved by the Ethics Committee of the Azienda Ospedaliera Universitaria Integrata of Verona and of the ERC and conducted in accordance with the 2012-13 Declaration of Helsinki.

2.1.1. Patient LF

LF (female, 49 years old, right-handed) has a left superior quadrantanopia (Fig. 1A) as a consequence of an ischemic stroke. The lesion involves the cortex of the anterior half of the right calcarine fissure up to the origin of the parieto-occipital fissure (Fig.1B). The patient was tested 30 months after the ischemic event.

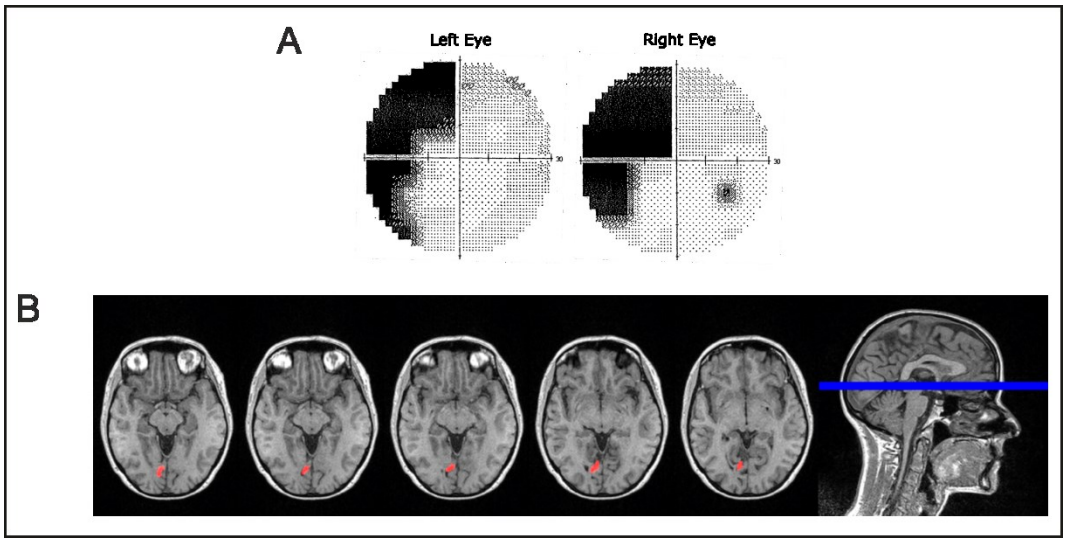

Figure 1. Patient LF: A) Visual field defect. B) Reconstruction of the lesion.

2.1.2. Patient LC

LC (male, 66 years old, right-handed) has a left homonymous hemianopia (Fig. 2A) due to a right temporal and parietal lesion, with posterior extension to the white matter of occipital lobe, involving the lateral part of optic radiation. (Fig. 2B).The patient was tested 17 months after the ischemic event.

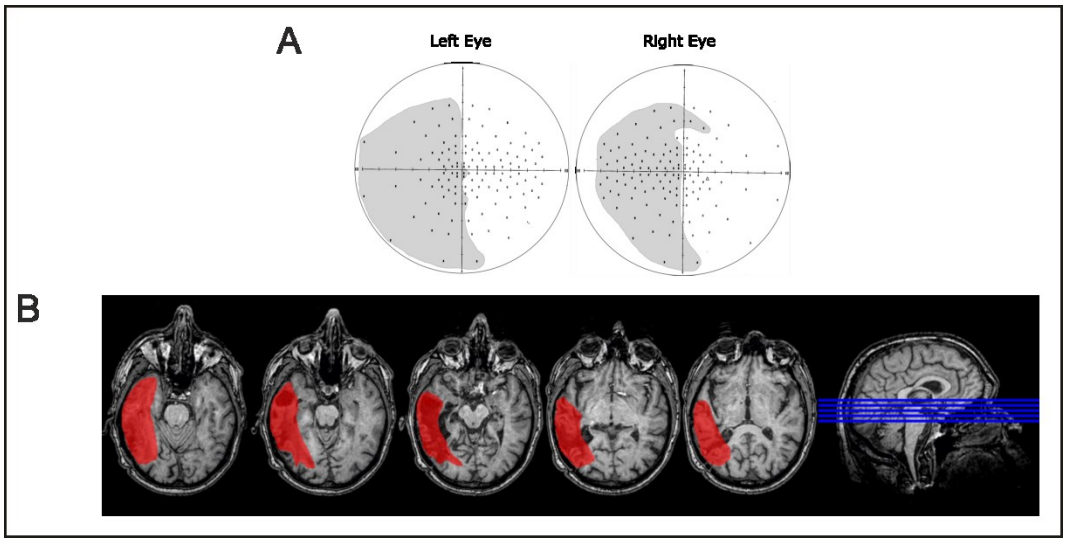

Figure 2. Patient LC: A) Visual field defect. B) Reconstruction of the lesion.

2.1.3. Patient GA

GA (male, 60 years old, right-handed) has a right inferior quadrantanopia (Fig. 3A) as a consequence of an ischemic lesion involving the left parieto-occipital lobe. In the occipital lobe, laterally, the lesion involves the superior, middle, inferior, and descending occipital gyri. Medially, the lesion involves the cuneus and the occipital pole, with relative sparing of the lingual and fusiform gyri (Fig. 3B).The patient was tested 11 months after the ischemic event.

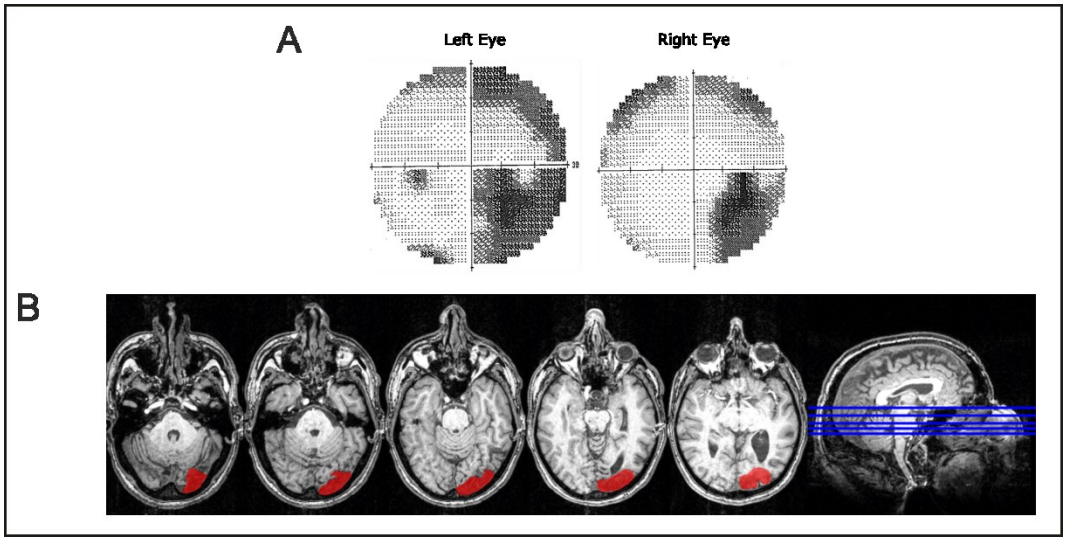

Figure 3. Patient GA: A) Visual field defect. B) Reconstruction of the lesion.

2.1.4. Patient AM

AM (male, 65 years old, right-handed) has an altitudinal hemianopia in his upper visual field (Fig. 4A), due a bilateral median para-sagittal occipital ischemic lesions involving the lingual gyrus, more evident in the right side where is visible a thinning of the anterior portion of calcarine cortex (Fig. 4B).The patient was tested 35 months after the ischemic event.

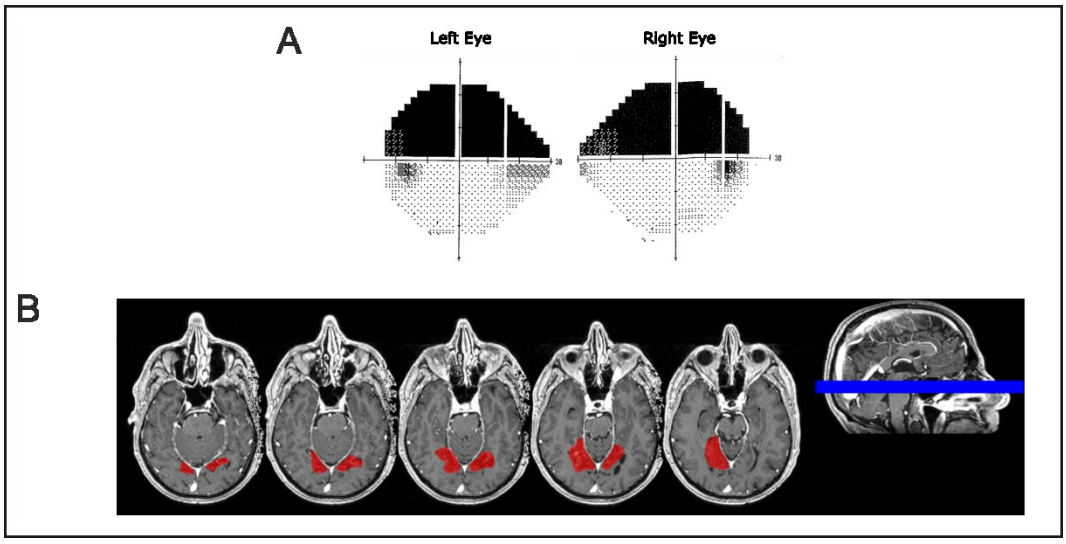

Figure 4. Patient AM: A) Visual field defect. B) Reconstruction of the lesion.

2.1.5. Patient SL

SL (female, 47 years old, right-handed) has a right homonymous hemianopia with partial foveal and upper hemifield sparing (Fig. 5A) as a consequence of an ischemic stroke with haemorrhagic evolution. The lesion involves the median para-sagittal portion of the left occipital lobe including the lingual gyrus, with peri-calcarine fissure distribution (Fig. 5B). The patient was tested 69 months after the event.

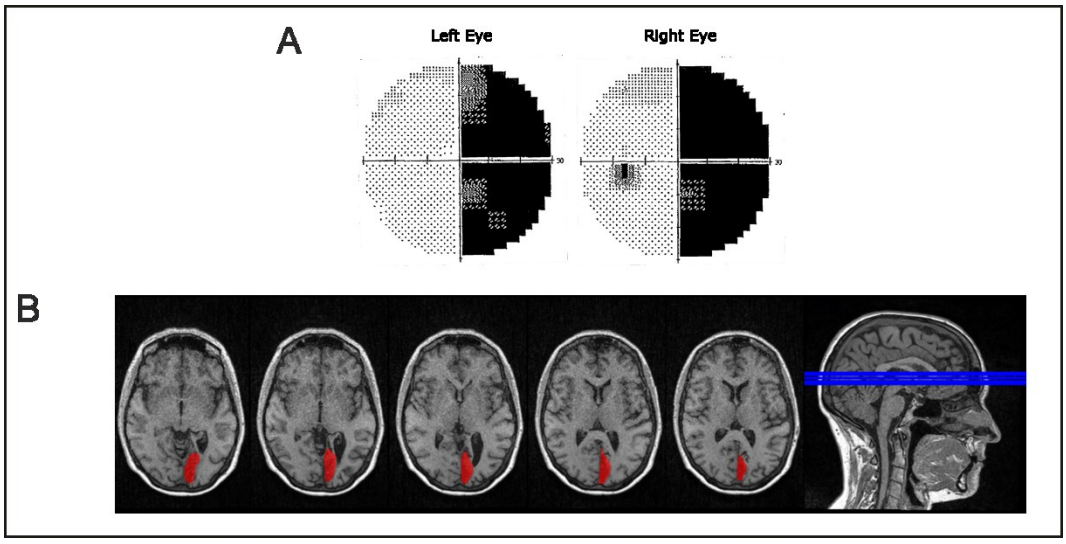

Figure 5. Patient SL: A) Visual field defect. B) Reconstruction of the lesion.

2.2. Behavioural procedure and statistical analysis

The behavioural procedure was the same as that used with healthy participants in Chapter 1 with the exception of the stimulus position. The stimulus position was chosen according to each patient visual defect. Each patient carried out preliminary testing to assess the visual defect. Patient AM performed the task in each quadrant to evaluate both upper and lower visual field. In summary, the eccentricity used for the stimulus presentation with patients was: Patient LF: 13° horizontally and 7° vertically; patient LC: ±16° horizontally, -7° vertically; patient GA: ±15° horizontally, -7° vertically; patient AM: ±6° horizontally, ±6° vertically and patient SL: ±16° horizontally, 7° vertically, measured from the inner portion of the display to the central fixation. For statistical analysis, we used a two-tailed binomial test, which allowed assessing if performance in the blind hemifield was significantly higher than chance level (50%). Two binomial tests were performed, one for the motion condition and one for the static condition.

2.3. EEG recording and analysis

The EEG recording procedure and the pre-processing of EEG data were the same as those used with healthy participants in Chapter 1.To assess the ERP responses of patients in the blind field and differences among the experimental conditions; a single-case analysis procedure was adopted. Percentile Bootstrap re-sampling (Efron and Tibshirani, 1993) was drawn on each trial of every condition of a patient. The percentile bootstrap method uses surrogate tests, which consist of randomly re-sampling with replacement for 5000 times the original trials among the conditions to create a data distribution from the shuffled data. Surrogate tests have the advantage to make no assumptions about the data. The bootstrap simulation allowed estimation of the patient sampling distribution adapted to any shape suggested by the data, taking into account variance and skewness of the sample. Next, point-by-point ANOVAs or T-tests were performed on all channels with the bootstrap data in order to identify differences between catch trials and the moving and static condition. The false discovery rate (FDR) correction (Benjamini and Yekutieli, 2001) was applied to

correct for multiple comparisons. In addition, ERP envelope (i.e. minimum and maximum of all electrodes at every time point) was used to calculate which IC gave the largest source contribution to the EEG signals in term of PVAF. With this procedure, we selected the IC or ICs that maximally accounted for variance at the electrodes in patient blind field. Lastly, in order to better understand the dynamics that underlie the generation of the ERPs in the blind field we used a source reconstruction based on an empirical Bayesian approach. The estimation of the current sources of the ERP components was carried out by using the Statistical Parametric Mapping software (SPM12 of the Wellcome Trust Centre for Neuroimaging, UK). The patient individual T1-weighted structural MRI image was used. The forward computation to prepare the lead field for the subsequent inversions was performed using the boundary element method (EEG-BEM) that create closed meshes of triangles with a limited number of nodes by approximating the compartments that conform the volume conductor (Fuchs et al., 2001). Successively, the inverse solution was computed on the entire ERP period after stimulus onset (i.e. from 0 to 800 ms) by using coherent smooth prior method (COH) (Friston et al., 2008) smoothness prior similar to LORETA (Pascual-Marqui, 2002). Sources in each time window of interest were visualized in terms of maximal intensity projection (MIP) with the corresponding MNI coordinates.

3. Results

3.1. Patient LF

3.1.1. Behaviour

In the intact hemifield field LF performance was comparable both in accuracy and RT to that of healthy controls (right static=99.4%, RT = 608 ms; right moving=99.5%, RT = 552 ms).In the blind hemifield LF performed at chance level with 53.9% (p=0.426) correct responses for static stimuli and 41.06% correct responses for moving stimuli (p=0.089) (Fig.6). She did not report any visual sensation upon stimulus presentation.

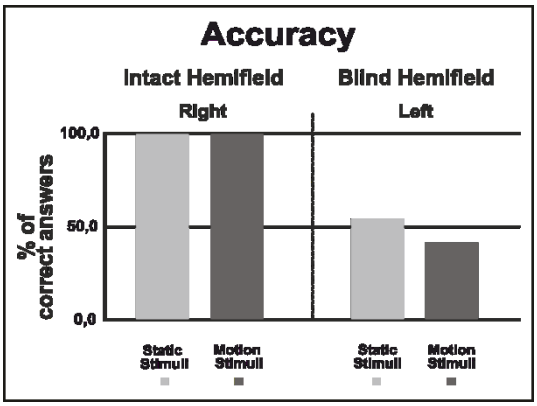

Figure 6. Patient LF: Behavioural results - Percentage of correct responses in each hemifield for each condition.

3.1.2. EEG

Blind Hemifield

Fig. 7 shows the ERP responses as recorded at electrode P3 (intact hemisphere) and P4 (damaged hemisphere) for the two hemifields and the three stimulation conditions. As can be seen from Fig.7 there are no reliable ERP responses when the stimulus was presented in the blind field, in keeping with the performance of the patient that was at chance level and without any stimulus-related sensation. A bootstrap ANOVA did not yield any difference between stimulus present and stimulus absent (catch) (all p-value were above 0.05 without multiple comparisons correction).

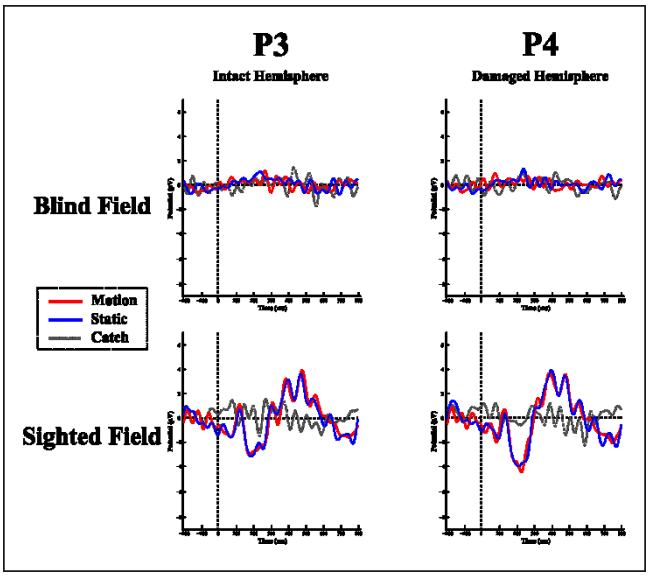

Figure 7. Patient LF: ERPs in the blind (top) and sighted field (bottom) as recorded at P3 (left-intact hemisphere) and P4 (right-damaged hemisphere) for the three stimulation condition.

Intact Hemifield

In contrast, when the stimulus was presented in the intact hemifield ERP responses were similar to those of healthy participants both in latency as well as in amplitude (Fig.7 bottom panel).

3.2. Patient LC Results

3.2.1. Behaviour

In the intact hemifield field LC performance was comparable in accuracy to that of healthy controls (right static=95.3%, RT = 608 ms; right moving=97.2%, RT = 552 ms), even he was slower in RT (right static= 989 ms; right moving= 1016 ms. In the blind hemifield LC performed at chance level with 58.1% (p=0.133) correct responses for static stimuli and 55.3% correct responses for moving stimuli (p=0.368) (Fig.8). He did not report any visual sensation upon stimulus presentation. Furthermore, it is important to highlight that the patient LC showed many missed responses (42%) in the blind hemifield.

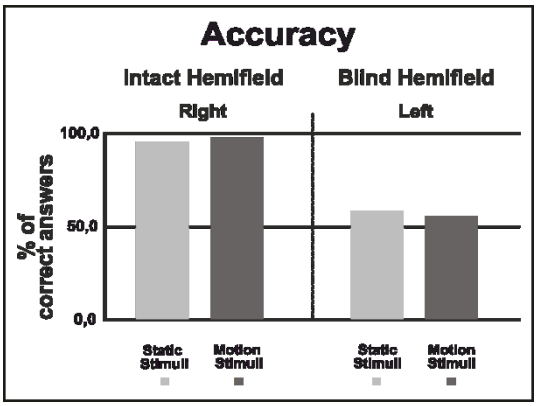

Figure 8. Patient LC: Behavioural results - Percentage of correct responses in each hemifield for each condition.

3.2.2. EEG

Blind Hemifield

Fig. 9 shows the ERP responses as recorded at electrode P3 (intact hemisphere) and P4 (damaged hemisphere) for the two hemifields and the three stimulation conditions. As can be seen from Fig.9 there are no reliable ERP responses when the stimulus was presented in the blind field, in keeping with the performance of the patient that was at chance level and without any stimulus-related sensation. A bootstrap ANOVA did not yield any difference between stimulus present and stimulus absent (catch) (all p-value were above 0.05 without multiple comparisons correction).

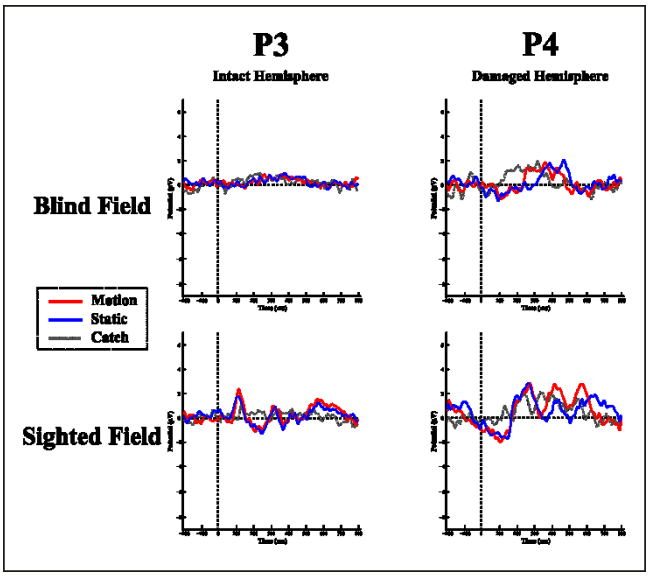

Figure 9. Patient LC: ERPs in the blind (top) and sighted field (bottom) as recorded at P3 (left-intact hemisphere) and P4 (right-damaged hemisphere) for the three stimulation condition.

Intact Hemifield

When the stimulus was presented in the intact hemifield ERP responses were very noisy (Fig.9 bottom panel), this is in keeping with the fact that he was under medication (with antiepileptic drugs) and the very large lesion. However, we found that P1 and N1 were similar to those of healthy participants both in latency as well as in amplitude. It is important to notice the absence of a clear P300. It has been demonstrated that cortical generator for this ERP component it is in tempo-parietal locations (for a review see Linden, 2005). In our patient, these areas are clearly compromised by the lesion, and this can explain the absence of P300.

3.3. Patient GA Results

3.3.1. Behaviour

In the intact hemifield field GA performance was comparable both in accuracy and RT to that of healthy controls (left static=98.6%, RT = 759 ms; left moving=95%, RT = 767 ms).In the blind hemifield GA performed at chance level with 47.9% (p=0.764)

correct responses for static stimuli and 60% correct responses for moving stimuli (p=0.057) (Fig.10). Interestingly, he reported a visual sensation upon stimulus presentation, declaring, "I know that the something was presented but I don't know what it was like."

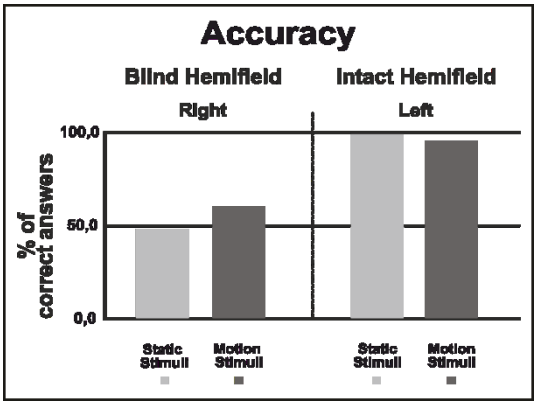

Figure 10. Patient GA: Behavioural results - Percentage of correct responses in each hemifield for each condition.

3.3.2. EEG

Blind Hemifield

Fig. 11 shows the ERP responses as recorded at electrode P3 (intact hemisphere) and P4 (damaged hemisphere) for the two hemifields and the three stimulation conditions. As can be seen from Fig.10 there are no reliable ERP responses when the stimulus was presented in the blind field, in keeping with the performance of the patient that was at chance level even though he reported a visual sensation. A bootstrap ANOVA did not yield any difference between stimulus present and stimulus absent (catch).

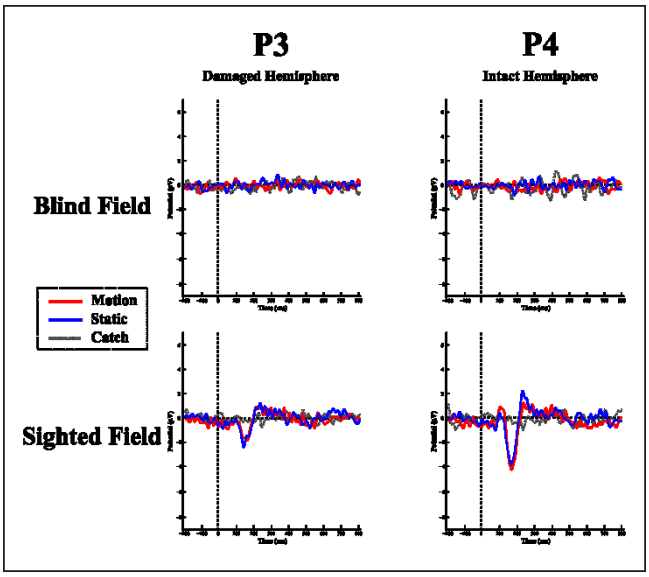

Figure 11. Patient GA: ERPs in the blind (top) and sighted field (bottom) as recorded at P3 (left-damaged hemisphere) and P4 (right-intact hemisphere) for the three stimulation condition.

Intact Hemifield

In contrast, when the stimulus was presented in the intact hemifield ERP responses were similar to those of healthy participants both in latency as well as in amplitude (Fig.11 bottom panel).

3.4. Patient AM Results

3.4.1. Behaviour

In the intact hemifield field AM performance was comparable both in accuracy and RT to that of healthy controls (right inferior static=100%, RT = 728 ms; right inferior moving=93.4%, RT = 653 ms left inferior static=97.8%, RT = 692 ms; left inferior moving=98.9%, RT = 632 ms).In the superior blind hemifield AM performed at chance level with static stimulation in both right hemifield, with 51.6% (p=0.764) of correct responses, and in the left hemifield, with 59.7% (p=0.057) of correct responses. Instead, in the motion condition his performance was at chance level just in the right hemifield with 49.3% of correct responses (p=0.920) (Fig. 12, left panel),

while he was statistically above chance in the left hemifield with 67.2% of correct responses ($p<0.001$) (Fig.12, right panel). Moreover, he reported visual sensation upon stimulus presentation in both hemifields without reporting any stimulus feature.

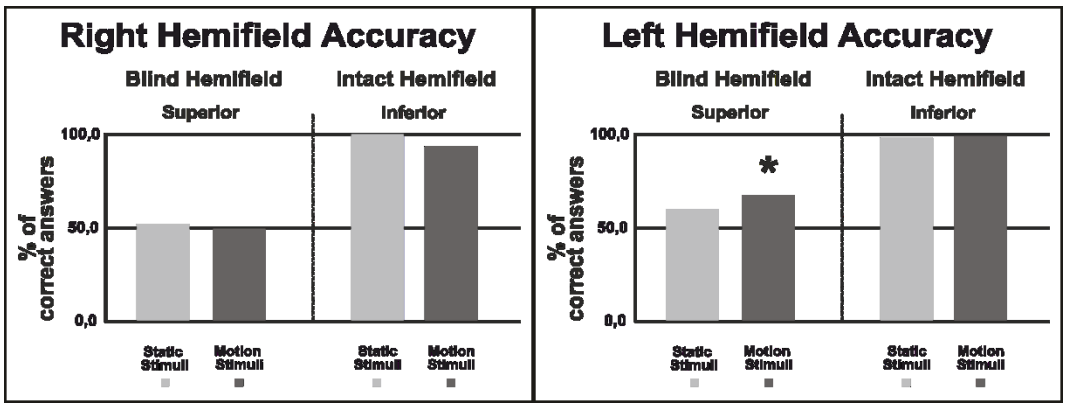

Figure 12. Patient AM: Behavioural results - Percentage of correct responses in each hemifield for each condition. Left panel: the stimulus was presented in the right hemifield. Right panel: the stimulus was presented in the left hemifield. The asterisk indicates that the number of correct responses was significantly different from the chance level of 50% ($p<0.001$).

3.4.2. EEG

Blind Hemifield

Fig. 13 shows the ERP responses as recorded at electrode P3 and P4 for the two hemifields and the three stimulation conditions. In the left hemisphere, there was a response when the stimulus was presented in the right hemifield. By the same token, in the right hemisphere there was an evoked response when the stimulus was presented in the left hemifield. The top panels show the response in the blind field while the bottom panels show the evoked response when the stimulus was presented in the intact field (inferior). As can be seen from top panel of Fig. 13, there are no reliable ERP responses when the stimulus was presented in the blind field even though the patient's performance was above-chance and he reported a visual sensation. Indeed, the bootstrap ANOVA did not reveal any difference between stimulus present and stimulus absent (catch) (all p-value were above 0.05).

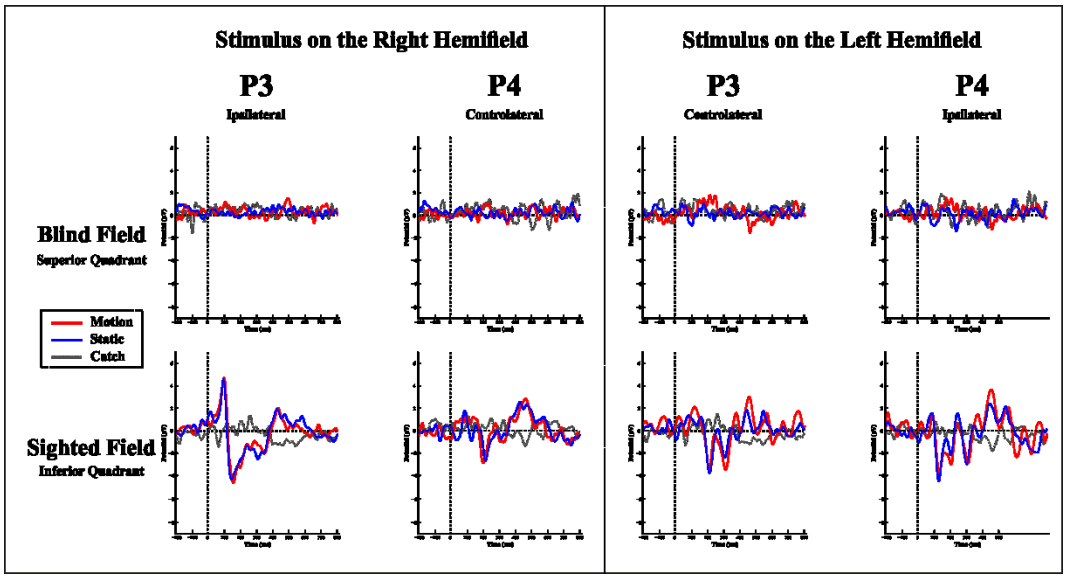

Figure 13. Patient AM: ERPs in the blind (top) and sighted field (bottom) as recorded at P3 (left-damaged hemisphere) and P4 (right-intact hemisphere) for the three stimulation condition when the stimulus was in the right hemifield (left panel), and when it was presented in the left hemifield (right panel).

Intact Hemifield

In contrast, when the stimulus was presented in the intact field ERP responses were similar to those of healthy participants both in latency as well as in amplitude (Fig.13 bottom panel). The polarity difference in the first peak of the intact fields (both left and right) is it in line with previous studies, which have demonstrated that the sign of C1 change according to a superior or inferior stimulus presentation in the visual field (Jeffreys and Axford, 1972).

3.5. Patient SL Results

3.5.1. Behaviour

The discrimination accuracy of patient SL in the intact hemifield was comparable both in accuracy and RT to that of healthy controls (left static=96.2%, RT = 531 ms; left moving=99.4%, RT = 577 ms). In contrast, she performed at chance level with static stimuli (55.03%; p=0.400) but with moving stimuli her performance was

significantly above chance with 65.56% correct responses ($p<0.005$) (Fig. 14). Interestingly, the patient reported "a feeling of something appearing in the blind field" during stimulus presentation without any idea of gratings' orientation or whether they were static or moving.

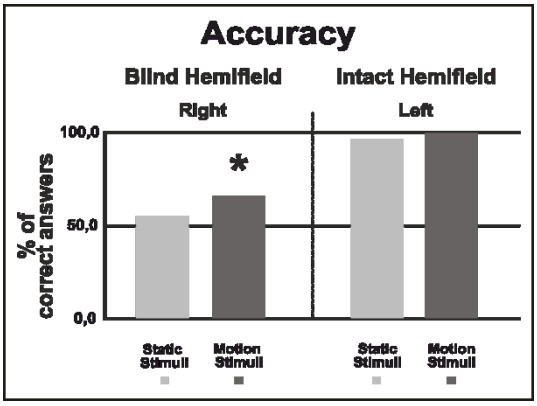

Figure 14. Patient SL: Behavioural results - Percentage of correct responses in each hemifield for each condition. The asterisk indicates that the number of correct responses was significantly different from the chance level of 50% ($p<0.005$).

3.5.2. EEG

Blind Hemifield

Fig. 15 shows the ERP responses as recorded at electrode P3 (damaged hemisphere) and P4 (intact hemisphere) for the two hemifields and the three stimulation conditions. In contrast to the other patients, visual inspection shows an early prominent negative component (N1) immediately followed by a positive (P2a) peak and later on by a long lasting negativity. The N1 is more pronounced in the damaged hemisphere.

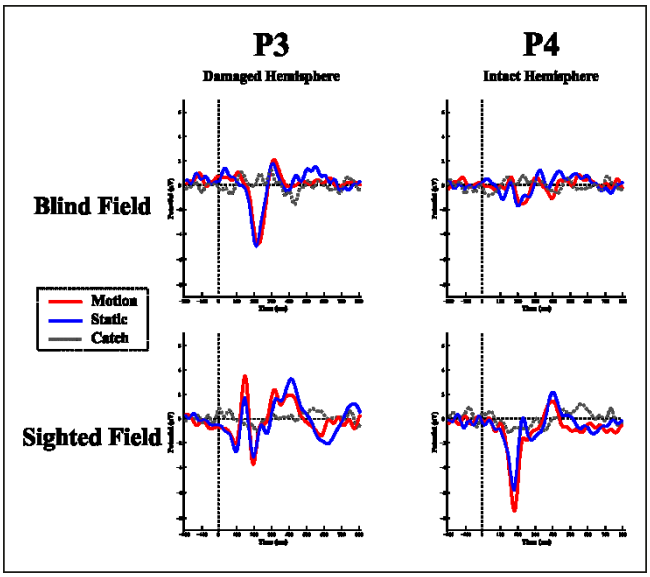

Figure 15. Patient SL: ERPs in the blind (top) and sighted field (bottom) as recorded at P3 (left- damaged hemisphere) and P4 (right- intact hemisphere) for the three stimulation condition.

Overall Scalp Distribution. Fig. 16 shows the overall scalp distribution of responses for the two hemifields of SL. As mentioned above, a large negative peak (N1) is clearly visible between 180 and 260 ms after stimulus onset. It is present both for static and moving stimuli and is widespread across left hemisphere electrodes with a larger amplitude with respect to the right hemisphere. It is important to underline the absence of the early ERP components C1 and P1 and also of the later component P3. Immediately after the early negative frontal peak (N1), there is a positive component (P2a) visible in both hemispheres and a later component at posterior electrodes in the right hemisphere. Below we describe and analyse in detail these three components that index different aspects of the patient performance and subjective report.

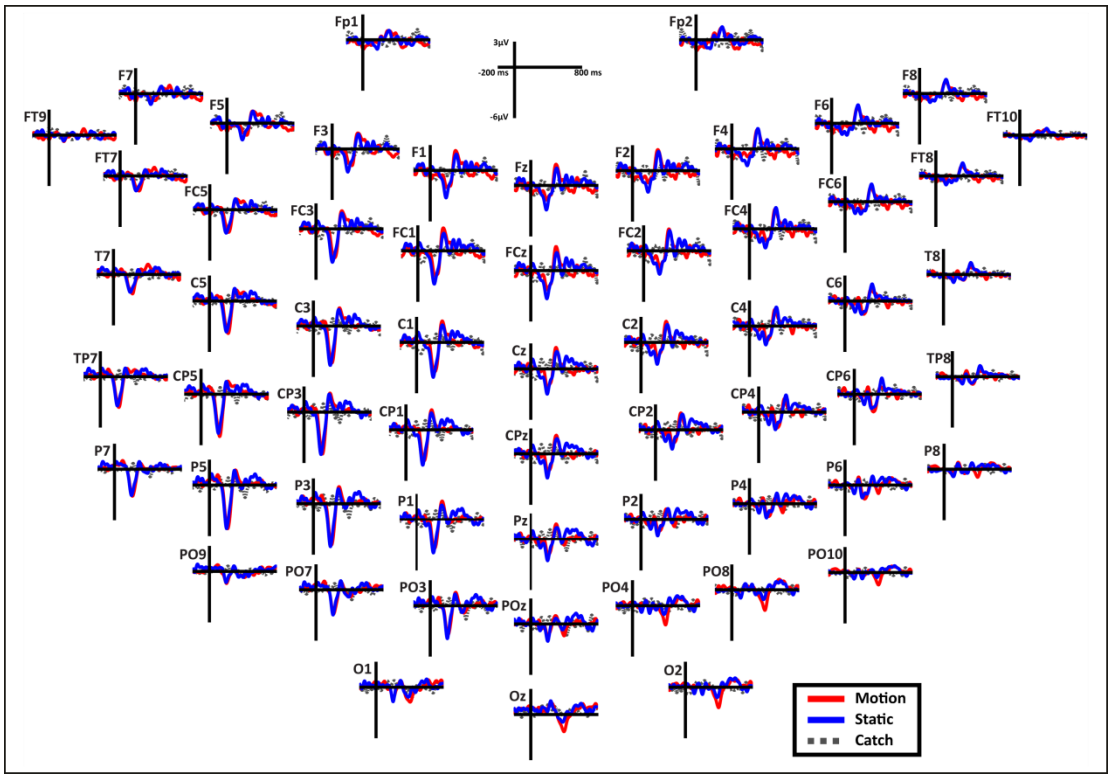

Figure 16. Patient SL: Scalp distribution of the ERPs when the stimulus is presented in the blind field. Note that the large negative peak (N1) is present in most electrodes in the left (damaged) hemisphere, while the frontal peak (P2a) is present in both hemispheres in the fronto-central electrodes. Finally, in the right posterior electrodes is present a late negativity selective for the motion stimuli.

N1. A bootstrap ANOVA was conducted for the three conditions of stimulus presentation (static, motion and catch). The main results are shown in Fig.17: Significant FDR corrected p-values ranged between 0.00084 and 0.04977. As shown by the raster plot the main difference between stimulus present and catch was in the N1 domain, in particular in the left posterior channels. In order to assess the reliability of the N1 peak two bootstrap t-tests were conducted: Moving vs catch condition and static vs catch.

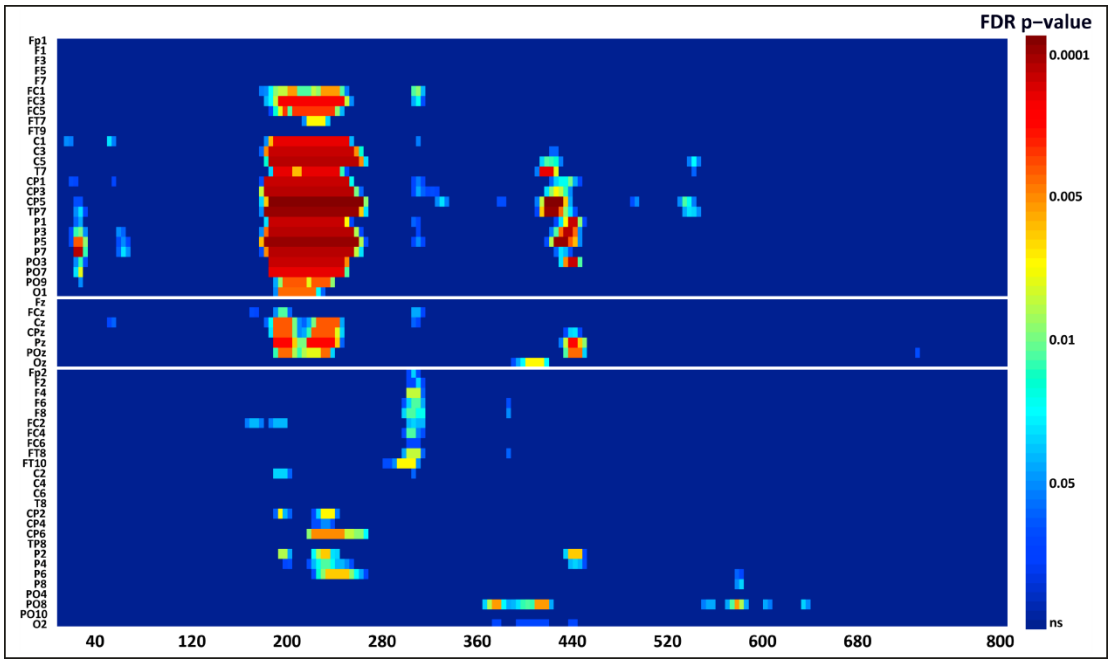

Figure 17. Patient SL: Raster data resulting from the bootstrap ANOVA across all electrodes and the three conditions of blind field stimulation. Colour points represent the p values after the FDR correction for multiple comparisons. Ordinates: left, electrode sites; right, p-values. Abscissae: post-stimulus onset time (ms).

As can be observed in Fig.18 the results of the two tests were very similar (all significant FDR p-values ranged between 0.00042 and 0.04430). An important point is that the N1 component was mainly present in the ipsilesional electrodes, i.e. contralateral to the blind hemifield in the damaged hemisphere, see Fig.16.

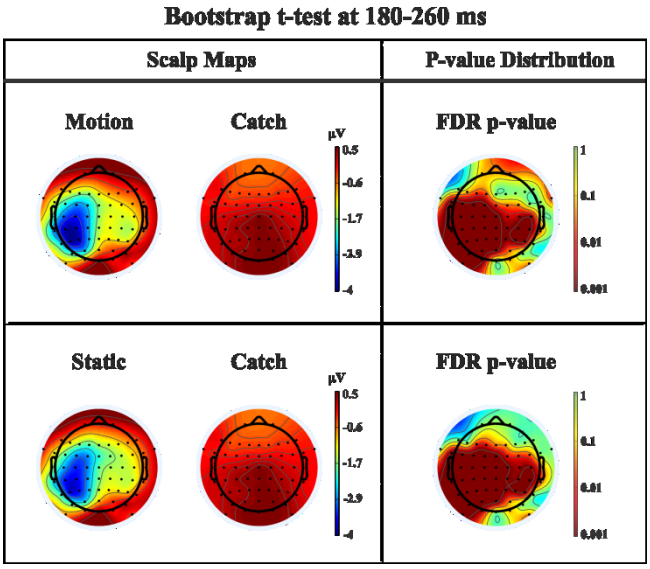

Figure 18. Patient SL: Percentile Bootstrap re-sampling t-test between stimulus against no-stimulus conditions in the time window of the N1. On the left side: Scalp maps representing motion against catch condition (upper panel) and static against catch condition (lower panel); Right side: distribution of the p-values after correction for multiple comparisons.

In order to examine its origin the PVAF (i.e. what percent of the scalp signal is reduced when a specific independent component IC is removed) was calculated from the ERP envelope for each condition of stimulus presentation (Fig. 19).

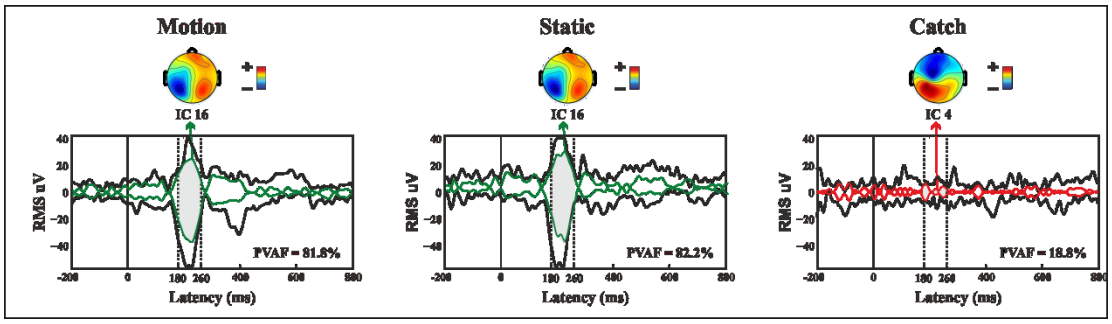

Figure 19. Patient SL: Envelope of the ERP (black line) for the three conditions of stimulus presentation to the blind field. The green line represents the contribution of the most prominent IC when the stimulus, either static or moving is presented. The red line represents the contribution of the most prominent IC during catch trials. The dotted lines represent the time window considered for the PVAF.

The result of this analysis showed that IC16 accounted for more than 80% of the ERP variance in that window; for the moving condition the PVAF was 81.8% with the maximum of variance at 224 ms; for the static condition was 82.2% with the maximum at 220 ms. For the catch condition the IC16 accounted only for the 4.4% of

the variance while the IC with the highest PVAF accounted for the 18.8% (IC4). Thus, IC16 was specifically involved in the generation of the N1 peak following stimulus presentation. Furthermore, we conducted a 3D source reconstruction in the time window of the peak. In this window the MIP was at MNI coordinates (-47, -79, 12), i.e. in the left extra-striate area, BA19, see Fig. 20.

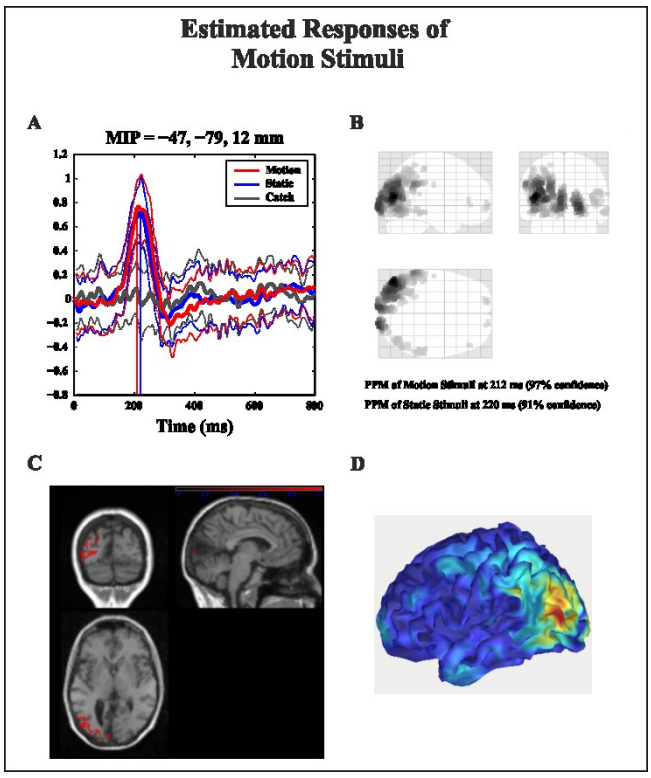

Figure 20. Patient SL: 3D source reconstruction of the ERPs when the stimulus was presented in the blind hemifield. A) Time course of the region with maximal activity for the three conditions. For both motion and static stimuli the MIP is at the same time (corresponding to N1 latency) in the extra-striate cortex (BA19). B) MIP of the 512 greatest source strengths within MNI space projected onto a glass brain for the motion condition. The area at the highest density corresponds to left BA 19. C) MIP of the statistical map for the motion condition projected on the T1-weighted images of patient SL showing both the lesion and in red the source reconstruction. D) Summary power image from source reconstruction of motion stimuli presentation to the blind hemifield on a 3D rendered image.

P2a. At left fronto-central electrodes, a significant positive peak was found immediately after N1, with a small amplitude and a latency between 250 and 320 ms after stimulus onset. It was present for both moving and static stimuli (the significant FDR corrected p-values for the motion condition against the catch ranged between 0.0031 and 0.0443 and those for the static condition ranged between 0.0061 and

0.0351), see Fig. 21. This component has a spatio-temporal distribution similar to a positive component referred to in the literature as anterior P2 (P2a: Potts et al., 1996; Potts and Tucker 2001; Brignani et al., 2009) or frontal P3 (P3f: Makeig et al.,1999) and also as frontal selection positivity (FSP: Kenemans et al., 1993; Martens et al. 2006). Indeed, its latency between 200 and 300 ms after stimulus onset, a positivity distribution in the frontal electrodes, and the fact that its peak emerges immediately after the N1 are similar to the typical characteristics of the P2a. Moreover, we found that this component was significantly different from catch trials for both motion and static stimuli.

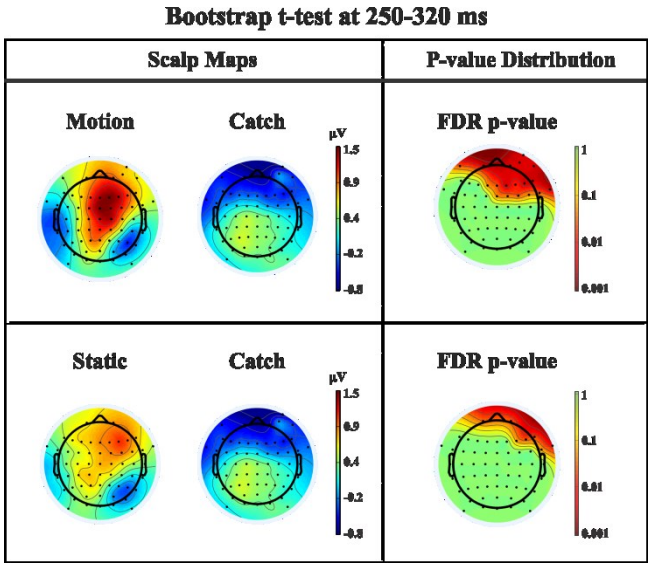

Figure 21. Patient SL: Percentile Bootstrap re-sampling t-test between stimulus against no-stimulus conditions in the time window of the P2a. On the left side: Scalp maps representing the motion against catch conditions (upper panel) and static against catch conditions (lower panel); Right side: distribution of the p-values after correction for multiple comparisons.

Late Posterior Negativity. Finally, an additional bootstrap t-test was conducted between static and moving trials in the time range of 320-440 ms (Fig. 22). This time window was chosen because of the presence of a negative peak in right posterior electrodes that was present only for the moving condition.

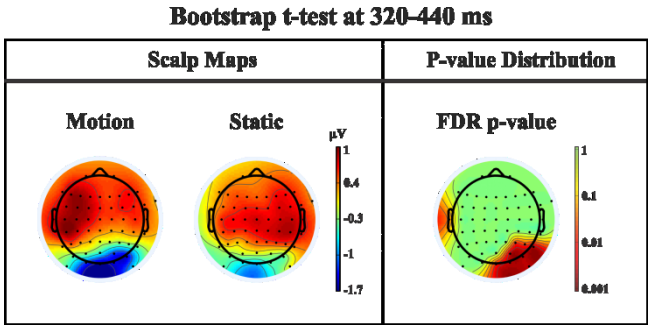

Figure 22. Patient SL: Percentile Bootstrap re-sampling t-test between Blind Motion and Blind Static conditions in the time window from 320ms to 440 ms. On the left side: Scalp maps representing the Bootstrap t-test to compare the motion against static; on the right side the distribution of the p-values after the correction for multiple comparisons.

The results showed a significant difference between static and motion conditions for posterior right channels (P4, P6, P8, PO4, PO10, and Oz) as well as T7 in left hemisphere (significant FDR corrected p-values ranged between 0.0024 and 0.0175). The envelope in this time window, see Fig. 23 showed that the IC accounting for most of the variance was IC16 with PVAF of 49.4% in the moving condition, while in the static condition its contribution was negligible (PVAF -3%).

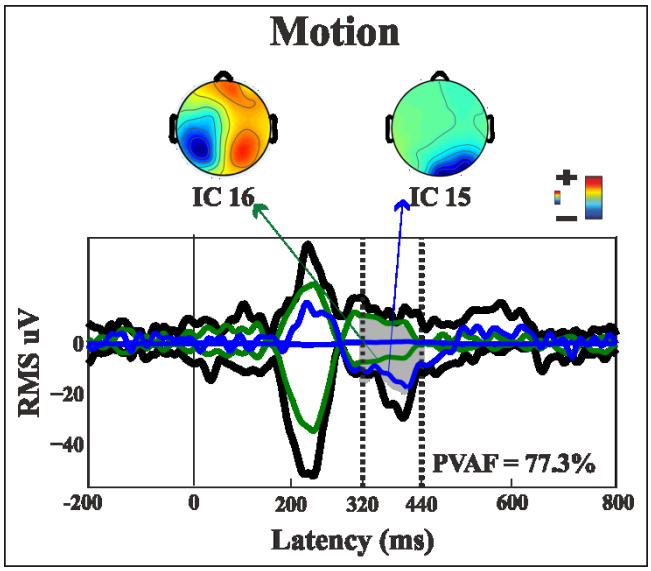

Figure 23. Patient SL: Envelope of the ERP (black line) for the motion condition of stimulus presentation to the blind field. The green and blue lines represent the contribution of the two most prominent ICs. The dotted lines represent the time window considered for the PVAF.

Intact Hemifield

The patient's ERPs when the stimulus was presented in the intact hemifield were similar to healthy participants in latency as well as in amplitude (Fig.15, bottom panel). Notice the presence of a large P3 component in the contralateral hemisphere.

4. Discussion

The present study aimed at exploring the neural correlates of conscious and unconscious vision in hemianopic patients. The main thrust of this study is that the patients' behaviour and report change on the basis of different lesion location. We found two patients (SL, AM) out of five that showed a significant above-chance performance and three (SL, AM, GA) that reported a sort of residual conscious vision. It is important to underline that only patient SL showed evidence of above-chance behavioural performance and visual sensation for the stimulus presentation, which correlated with ERPs responses (Late posterior negativity and N1-P2a).

In this patient, we found three different ERP components that are related to her behaviour and subjective report: the N1 and P2a are related to her degraded conscious vision while the late posterior negativity is related to the above-chance performance.

N1-P2a components. As described in the Results, patient SL upon stimulus presentation in the blind hemifield reported that she had no clue as to the features of the stimuli, i.e. about their orientation or whether they were static or moving. However, she was consistent in discriminating catch from stimulus trials, as reported in preliminary testing and in another study (Mazzi et al., 2016), and after each trial block in reporting the occurrence of the stimuli as "something appearing in the visual field". In contrast, the other hemianopic patient LF never experienced the presence of the stimuli or a difference between catch and real trials. An important finding is a clear correspondence between the subjective reports of the two patients and their electrophysiological responses to stimuli presented to the blind field. Patient LF did not provide any perceptual report while in SL two ERP components can be

considered as likely correlates of her report, namely N1 and P2a, i.e. the frontal positive peak immediately following N1. Both components were present irrespective of whether the stimuli were static or moving and therefore cannot be considered as related to the behavioural evidence of orientation discrimination but rather to the "feeling that something appeared in the blind field." The time window of the N1-P2a components is roughly compatible with that of the Visual Awareness Negativity (VAN) that is, a ERP component resulting from the difference between conscious and unconscious stimulus processing (Koivisto and Grassini, 2016; Koivisto et al., 2016). Notably, the electrode location where the N1 was clearly detectable was widespread in the ipsilesional hemisphere, see Fig. 6. Its source could be located mainly in the left extrastriate cortex (BA 19) and, to a lesser extent, in the right hemisphere. It is important to underline that, in contrast to N1, the early components, C1 and P1, and the later component, P300, were absent following blind field stimulation. The absence of C1 and P1 might explain the incapacity of SL to discriminate the orientation of static stimuli and is a likely consequence of the striate cortex lesion impairing initial basic sensory processing with static stimuli. In healthy subjects, the N1 was followed by a small amplitude complex P2-N2 and by a very large P300 while this was not the case in SL. This is in keeping with SL lack of full stimulus awareness. Thus, we believe that the presence of N1 and P2a might be considered as an electrophysiological correlate of degraded conscious vision. This possibility is reinforced by the source of N1 in BA 19 which is broadly in agreement with Bagattini et al., (2015), Koivisto and Grassini (2016) and Tagliabue et al., 2016, and with the hypothesis of an early site of emergence of perceptual awareness. In the present case, however, it is awareness of degraded rather than full vision. The relationship between N1 and perceptual awareness is controversial. On one hand N1 has been repeatedly associated with selective attention, see Mangun (1995), rather than with consciousness. In keeping with that, Sergent et al. (2005) in an attentional blink paradigm found that the presentation of unseen words yielded a P1 and N1 component prior to emergence of consciousness that occurred at later processing stages. On the other hand, there is evidence for a link of N1 with awareness. For

example, in a face inattentional blindness paradigm Shafto and Pitts (2015) found that the N170 was absent during inattentional blindness and present in the aware conditions. Studies of binocular rivalry have also provided important information on the physiological correlates of consciousness. For example, Kaernbach et al., (1999) and Roeber and Schroeger (2004) have shown that changes of perceptual awareness are witnessed by changes of the N1 component and this is in accord with an early emergence of consciousness probably made possible by feedback processes involving V1, see Di Lollo et al. (2000); Lamme and Roelfsema (2000); Tong (2003). Thus, although debated, the involvement of N1 in an early onset of perceptual awareness seems to have solid grounds.

Late posterior negativity. Starting from the historical finding by Riddoch (1917) who provided evidence of residual degraded vision for moving stimuli in cortically blind patients (Zeki and ffychte, 1998), that motion stimuli are the most frequent protagonists of above chance unconscious discrimination (blindsight type 1) is a well-established notion, see Ajina and Bridge, 2016 for a recent review and Azzopardi and Cowey (2001) for controversial evidence. In the present study, the novel finding is that the presence of motion made possible the above-chance discrimination of another visual feature, namely pattern orientation. Patient SL was able to discriminate orientation only when the gratings drifted either horizontally or vertically. This effect might be attributed to activity of cortical motion area V5/MT receiving input from subcortical centres bypassing V1 (Ajina et al. 2015; Kavcic et al., 2015) and retaining the capacity of discriminating apparent motion in the absence of V1. Importantly, the ERP results in patient SL showed a difference between the static and the motion condition in the posterior electrodes of the intact right hemisphere, see Fig. 13, as a negative peak around 390 ms post stimulus onset. The PVAF analysis showed that this peak could be accounted for by the same ICs as for the N1 but bilaterally distributed and is in agreement with V5/MT activity. Thus, moving stimuli engage large neuronal pools that enable an effective interhemispheric transfer of directional movement information presumably at parietal level. In keeping with this possibility is

the finding in the present study of ERP differences between moving and static stimuli in the right hemisphere of healthy controls. In addition, these results are in accord with Kavcic et al. (2015) who found an interhemispheric transfer of motion information in hemianopic patients with left but not right hemisphere damage. Indeed, one likely possibility is that the blindsight exhibited by patient SL is subserved by the intact (right) hemisphere as a result of interhemispheric integration and this is in broad agreement with the results of Celeghin et al. (2015a) who found that in hemianopic patients the above-chance visuo-motor responses in a simple RT paradigm depended on the intact hemisphere as a result of interhemispheric transfer.

It is important to notice that another patient showed a similar behaviour as patient SL. Patient AM reported both experience of the stimulus and an above-chance performance. As for patient SL performance was above-chance just for moving stimuli even though perceptual awareness was present for both stimulus conditions. Interestingly, because of AM altitudinal hemianopia it was possible to analyse both blind hemifields and we found an interesting difference: only the stimulus presented in the left hemifield showed above-chance performance. This difference could be explained by the left hemisphere's larger damage compared with that of the right hemisphere. By the way, it is important to highlight that despite similar behaviour it was not possible to find any EEG correlates in response to blind field stimulation, as in patient SL. Also patient GA reported a visual sensation of the stimulus when it was presented in the blind field but his performance was at chance level for both stimulus conditions, even though he showed a trend to be more correct in the motion condition. Also in this case we could not find any reliable response in EEG recording following blind hemifield stimulus presentation.

5. Conclusion

In conclusion, we found reliable EEG responses in a hemianopic patient with a selective lesion of left V1 who showed an above-chance discrimination of the orientation of moving visual gratings presented to the blind hemifield. Importantly,

the patient reported no visual experience of the different features of the stimuli except for a visual sensation that something appeared in the blind hemifield. This subjective observation found an electrophysiological correlate in the presence of a N1 and of a frontal P2a component. In contrast, the earliest visual components such as C1 and P1 and the later P300 could not be identified. Thus, as to the earliest physiological correlate of perceptual awareness our results support an early stage occurrence. However, this conclusion applies to a form of degraded visual experience and might not necessarily be generalized to onset of full perceptual awareness. As far as the blindsight effect found for the discrimination of the orientation of moving stimuli, a very likely physiological correlate is represented by the posterior late negative component in the intact right hemisphere. It is important to stress that the behavioural performance of patient SL can be defined as a form of blindsight made possible by stimulus motion. In this study, another patient (with a bilateral lesion leading to an altitudinal hemianopia) showed both degraded vision and above-chance performance, but it was not possible to find any EEG correlate. Also, patient GA showed a visual sensation similar to that of patient SL but without any EEG correlates. The absence of a reliable ERP response could be explained by the different size and location of the lesion that are larger in patients GA and AM compared with patient SL. Finally, one should note that patient SL underwent a stroke almost six years before the present testing and that this suggests the possibility of plastic neuronal reorganization of her cortical and subcortical areas while for patients GA and AM the recording took place only less than one year from the event for GA and less than three years for AM. It is possible that this time probably is not sufficient to obtain some cortical reorganization as in patient SL. It would be interesting to gather further information in future testing session to find out whether this reorganization is still in progress and might further enable a shift from totally or partially unconscious behaviour to full perceptual awareness.

- **Part II: Neural correlates of short-term memory and resting state**

Chapter 3
Individual differences in resting state connectivity and their relationship with short-term memory

1. Introduction

The internal representation of the external world relies on our capacity to hold in mind various amounts of information. This capacity is what is known as short-term memory (STM). Temporary storage abilities, such as STM and working memory (WM) are considered a stable characteristic of intellectual and cognitive functions. However, it has been demonstrated that there is a great individual variability in STM performance, which is closely related to differences in fluid intelligence and cognitive aptitudes (Engle et al., 1999; Cowan et al., 2005; Fukuda et al., 2010). This variability is also probably reflected in the organization of brain cortical architecture, which is fundamental to carry out complex cognitive tasks. It is a well-established fact that there is an overlap between STM and cognitive control (Awh and Jonides, 2001; Gazzaley and Nobre, 2012) that optimizes perception by enhancing detection and discrimination of relevant targets and by suppressing irrelevant information (for a review see Desimone and Duncan, 1995). The involvement of a cognitive control system can explain why STM performance in different cognitive domains tends to be correlated (Stevens et al., 2012). Many studies have demonstrated the involvement of fronto-parietal areas in STM tasks (Mayer et al., 2007; Rutman et al., 2010). The role of these areas is to maintain the information, independently from the kind of sensory modality; therefore, they should receive a direct or indirect input from the domain-specific posterior lower-level sensory areas, which encode the information to be memorized. Thus, in order to better understand the dynamics underlying STM it is important to study the interactions among the multiple brain areas usually engaged in

STM tasks. In particular, it is of great importance to study the STM mechanisms and dynamics responsible of the great variability among subjects. This variability is likely to be generated by inter-individual differences in the connections between the fronto-parietal system and the lower-sensory areas. We hypothesize that this variability can be reflected in the functional connectivity of the networks involved in STM, even when the subject is not actively involved in a memory task.

In the last decade, a growing body of neuroimaging research has demonstrated that the cerebral spontaneous activity is spatially and temporally structured in networks, the so-called resting-state networks, (RSNs), challenging longstanding assumptions that this activity is just internal noise. It has been hypothesized that RSNs represent the spatio-temporal correlates of past experiences and the prediction of the response to upcoming stimulations (Engel et al., 2001; Friston, 2002; Deco and Corbetta, 2014). Many studies have demonstrated that intrinsic brain activity can predict trial by trial individual differences and variability in task performance (Fox et al., 2007; Kelly et al., 2006; Hampson et al., 2010), suggesting that the intrinsic functional connectivity of the cognitive control networks measured in a resting state paradigm provides substantial information about actual cognitive performance (Stevens et al., 2012).

So far, the favourite tool to investigate resting state has been fMRI, which is an indirect measure of brain activity as it is based on a hemodynamic response. Moreover, despite its good spatial resolution, fMRI has a poor temporal resolution in the order of seconds compared to milliseconds of EEG or MEG. In particular, the latter technique circumvents this problem because it relies on the magnetic field produced by the neural activity of the neurones. Many studies have used MEG power envelope to derive RSNs with results spatially similar to those found with fMRI (de Pasquale et al., 2010; Brookes et al., 2011; Hipp et al. 2012; Wens et al. 2014a, 2014b) but with a higher temporal resolution. These studies have provided evidence of the importance of exploring the temporal dynamics of the resting state in order to understand the connections among networks.

In the light of that, we decided to use MEG in our investigation because of its temporal resolution and because, when it is combined with an adequate inverse model, it allows a source reconstruction with good spatial resolution.

The aim of the present study is double: to confirm the feasibility and efficiency of MEG as tool to assess the RSNs by studying the temporal structure of spontaneous oscillatory activity; and, to verify if the variability of connectivity at rest can predict individual differences in STM capacity. In particular, we wanted to assess if the dynamics of the fronto-parietal networks and of the areas connected with them correlate with STM performance.

2. Methods

2.1. Participants

Eighty healthy participants aged between 17 and 34 years were recruited to participate in the study. Five subjects dropped out before the completion of the study[1], eight subjects were not MEG compatible for the presence of orthodontic appliances or other metallic materials; and 13 participants were excluded because over 50% of their data had to be removed due to high noise levels caused by movement and eye-blink artefacts. The final dataset includes data from 54 participants, (mean age = 24.09 years, SD= 4.43, 34 females). All subjects had normal or corrected-to-normal vision and no history of psychiatric or neurological conditions. All participants gave written informed consent for participation in the study that was approved by the University of Cambridge Psychology Research Ethics Committee.

[1] *This study was part of a larger study involving a training procedure, see Chapter 4*

2.2. Cognitive assessment

Multiple different short-term memory (STM) assessments were administered using a tablet computer. Verbal STM was evaluated using three tests: Forward Digit Span and Forward Letter Span required participants to recall sequences of visually presented digits or letters, respectively; the Forward Digit Span procedure was also administered with acoustically presented numbers. Spatial STM was evaluated using two tests: a Spatial Span Task, similar to Corsi blocks task (Corsi, 1972), required participants to remember locations of a sequence of dots for subsequent recall and a Visual Pattern task (Della Sala et al., 1997), that consists of a square grid with patterns of flashing squares presented simultaneously; subjects were required to remember the spatial arrangement. For all span tasks, the procedure was divided into blocks of six trials. The trails of the same block have the same series length. Each trial consists within a series (a set of items) to be remembered. If at the end of the block, the subjects got four or more correct trials they would get another block of six trials with a longer series (one extra memory item within each set). The task continued adding an extra item within the series for each block, until they scored less than four correct trials in a block. The length of the series prior to this unsuccessful final block determined the individual span for each task. The score was calculated as the proportion of correctly remembered trials weighted by this individually determined span. Visual STM was measured using two Visual Change-detection tasks (Luck & Vogel, 1997), with either coloured dots or oriented arrows as targets, with subjects deciding if the second array was identical or different from the first. In these tasks the number of item presented could be 6, 9, or 12. Each condition had fixed number of 20 trials. The score was calculated as the sum of the proportion correct for each of the three conditions.

2.3. Behavioural analysis

In order to establish the potentially different underlying memory processes that our battery assessed, we used a data-driven principal component analysis. We used a

varimax rotation, with the aim of maximizing the distinction between any potentially separable underlying factors. We identify three factors on the basis of eigenvalues. For the interpretation of the factor we used the factors that after the rotation showed an item loading greater than 0.45.

2.4. MEG data acquisition

Nine minutes of eyes-closed MEG resting state activity were continuously recorded in a magnetically shielded room using a VectorView MEG system (Elektra-Neuromag) that contains a magnetometer and two orthogonal planar gradiometers at each of 102 locations (totals of 306 sensors). The MEG activity was recorded at 1000 Hz sampling rate with a high-pass filter of 0.01Hz. A three-dimensional digitizer (Polhemus FASTRACK) was used to record around 100 head shape coordinates relative to the position of the five head position indicator (HPI) coils and the fiducials (the nasion and the left and the right preauricular points), which were used to monitor the head position during recording. Additionally, two bipolar electrodes recorded the ECG (electrocardiogram) pulse from wrists and four bipolar electrodes (HEOGs and VEOGs) recorded horizontal and vertical eye movements throughout the session. Subjects were instructed to sit comfortably, to close their eyes, to try to stay as still as possible without focusing on any particular thought or falling asleep.

2.5. MEG analysis

We used the same analysis pipeline of Barnes et al. 2016.

2.5.1. Pre-processing

The raw MEG data were processed offline using a combination of custom scripts written in FSL (FMRIB's Software Library, www.fmrib.ox.ac.uk/fs), SPM 12 (Wellcome Trust Centre for Neuroimaging, UK, www.fil.ion.ucl.ac.uk/spm/software/). As a first step, the raw data were processed using MaxFilter version 2.0 (Elektra-Neuromag) to reduce the strength of external noise (using a signal space separation method). The MaxFilter, in particular the

MaxMove algorithm, was used to compensate for head movement. The data were also downsampled to 250 Hz. Then, the continuous raw data were visually inspected and large artefacts resulting from signal jumps were rejected. At this stage, bad channels were also identified and removed, via visual inspection. In order to remove heartbeat and eye-movements artefacts a temporal Independent Component Analysis (ICA) was run at channel-space level, using fastICA algorithm. To identify the bad component we used a combination of metrics and manual inspection: components, which showed a correlation higher than Pearson r=0.1 with ocular and cardiac channels were removed.

2.5.2. Source reconstruction

Each subject's MEG data were co-registered to a standard MNI template using the digitized scalp locations and fiducials via an iterative closest point algorithm using SPM12 (http://www.fil.ion.ucl.ac.uk/spm/). Prior to beamforming the data were bandpass-filtered to focus only on the frequencies within the beta band (14-30 Hz); previous work has shown that these frequencies are best for exploring functional connections with MEG (Brookes et al. 2011; Barnes et al., 2016), and more generally that focusing on these oscillations increases the discrimination between spurious and genuine connectivity (Luckhoo et al. 2012). For each subject, source space activity was estimated at every vertex of an 8mm grid covering the entire brain, using a linearly constrained minimum variance beamformer (Van Veen el al., 1997). The beamformer combines information from both the magnetometers and planar gradiometers while taking into account the reduced dimensionality of the data introduced by the signal-space separation algorithm (Woolrich et al., 2011). Beamformer procedure works constructing a set of spatial filters, which are applied to the sensor data to reconstruct the signal at each grid point throughout the brain, with the aim of achieving unit bandpass response at the grid point while minimizing the contribution from all other sources. The process can be repeated across all grid locations to achieve a whole brain source reconstruction.

2.5.3. Amplitude Envelope Estimation, Down-sampling, and Concatenation.

Once we created the dataset that contained source-projected oscillatory data, we estimated the amplitudes of those oscillations through computation of the absolute value of the analytic signal, which was found using a Hilbert Transform. Basically, this procedure leads to an estimate of instantaneous signal amplitude at each voxel, at our frequencies of interest. The envelope time series for every voxel was then low-pass filtered and we divided each envelope time course into 1s windows and averaging within those windows (see Brookes et al., 2011). Both beamformer-weights-normalised and non-beamformer-weights-normalised envelopes were estimated for use in the subsequent group-level (general linear model) analysis (Luckhoo et al., 2014). Spatial smoothing was also applied to the down-sampled envelope estimates (FWHM 5mm).

Once we had down-sampled amplitude envelopes for all source space voxels and all subjects, we temporally concatenated the beamformer-weights-normalised envelopes across all participants to produce one continuous dataset that contained all participants' data, adjoined end-to-end.

We analysed the MEG resting state data in two ways. Firstly, we used a temporal ICA procedure to derive networks in our participants. Secondly, we identified three particular networks of interest, in this case using spatial information from an independent fMRI dataset, and then we extracted electrophysiological information from those networks using a dual regression procedure. Using this combined fMRI / MEG analysis, we could then explore functional connections between other brain systems and these networks on the basis of this electrophysiological information. Finally, we obtained whole-brain maps for each subject and used them to run a GLM, in order to find out whether differences in connectivity at rest are associated with individual differences in our cognitive measures.

2.5.4. Temporal ICA

To identify temporally distinct RSNs using the source-space envelope data we used a temporal Independent Component Analysis (ICA) as a blind source separation method. Substantially, this is a validation procedure, because it has been demonstrated that this approach can be used to derive RSNs using the spontaneous fluctuations in ongoing oscillatory signal (see Astle et al., 2015 and Barnes et al., 2016). This temporal ICA was run to reduce the data in 25 temporally independent components. To do that we combined the Principal Component Analysis (PCA) with the fastICA algorithm (Luckhoo et al., 2012). Each of the 25 independent time courses generated were converted into correlation spatial maps by estimating the Pearson correlation coefficient between each time course and the amplitude envelope associated with each voxel. This process was repeated across all vertices to yield a whole-brain map for each temporal IC. The maps created using this procedure correspond to our RSNs. This approach replicates that used by Brookes and colleagues (2011) and it identifies brain areas with oscillations that have a similar temporal structure. Then, we compared our networks to a set of canonical networks from an independent resting state fMRI study (Smith et al., 2009). To do that we calculated spatial cross-correlations (using *fslcc*, a special tool included in FSL library) between our MEG-derived networks and our canonical fMRI RSNs maps (Woolrich et al., 2009, as in Barnes et al. 2016). The spatial correspondence was calculated for seven different classic RSNs: the right fronto-parietal (rFPN), the left fronto-parietal (lFPN), the bilateral fronto-parietal, also known as dorso-lateral attentional network (DAN), the anterior cingulate (ACC), the visual, the sensori-motor and the cerebellum components.

2.5.5. MEG-adapted dual regression

In this study, we investigated whether variability in fronto-parietal RSNs would be related to individual differences in STM capacity. We used an independent set of canonical fMRI RSNs as a basis set for this analysis (Smith et al., 2012). The

advantage of choosing networks a priori from this independent data set is that it takes advantage from the higher spatial information in fMRI, providing a well-identified standard set of RSNs. Within this set of canonical RSNs, we then only looked for differences among subjects in the left and right lateral fronto-parietal and bilateral fronto-parietal networks. We chose these networks a priori because they represent our best approximation of those cortical networks particularly responsible for cognitive control. It is possible that better expression of, and / or communication with, these networks is associated with enhanced STM performance outside the scanner. We therefore tested whether differences in these networks, or in the areas that communicate with them, might explain individual differences in memory capacity.

In order to derive subject specific maps for each of the fMRI networks, we performed a MEG-adapted dual regression (DRMEG) analysis (Luckhoo, 2014), analogous to the dual regression approach developed for use in fMRI data (Filippini et al., 2008). In the first stage of DRMEG, we performed a spatial regression of the fMRI network maps on the concatenated beamformer-weights-normalised envelopes to yield concatenated network time courses. In the second stage, we broke these concatenated time courses into subject specific blocks. For each subject, we performed a temporal regression of the network time course segment from the non-beamformer-weights-normalised downsampled envelopes. By means of this procedure, we obtained a spatial map for each RSN that is specific to each subject, but definitely, the estimation of the true variance of activity for that network has an unbiased estimate, and this is primary for all subsequent multi-subject statistics (Luckhoo et al., 2014). The result of this methodology was that we obtained a whole-brain map for each subject and chosen network, which corresponded to each voxel's strength within that network.

2.5.6. Group level regression analysis (GLM)

The final stage of our analysis pipeline tested whether variability in our derived RSNs, or in the areas that communicate with them, correlate with STM performance. In order to do this we used a voxel-wise General Linear Model (GLM) (Friston et al. 1994) to establish significant associations between the spatial distribution of each network and the behavioural scores. The aim of GLM procedure is to explain or to predict the variability of a dependent variable in terms of linear regression using multiple regression procedure. In short, we used the following linear model:

$$Y = \beta_1 * Order\ STM + \beta_2 * Visuo\text{-}Spatial\ STM\ Factor + \beta_3 * Visual\ STM\ Factor + noise.$$

Where Y it is the connectivity at each voxel, while $\beta_1, \beta_2, \beta_3$ are the beta values that indicate the level of correlation for each regressor. The beta values from this model were then used to explore the neural impact of STM measures on ongoing brain activity. The outcome was that for each of our seed networks we had a whole-brain dataset in which we estimated the linear contribution of each of our behavioural factors to voxel-wise connectivity values (as indexed by the corresponding beta values from the model). We adopted a standard procedure for testing the hypothesis that there are no significant clusters of voxels. We identified clusters of contiguous voxels where the output of the voxel-wise GLM was greater than t=2.46. This value is essentially arbitrary since it is the subsequent permutation process that actually tests for significance. However, we chose this value because it takes into account our degrees of freedom, and is Bonferroni corrected to account for our GLM being repeated on three networks, and the alpha limit was split in two, to account of the two-tailed distribution. This threshold corresponds to a p value of 0.0083. Once we identified the size of these clusters, we conducted a sign-flipping permutation procedure to produce a null distribution, using 5000 permutations. We were then able to compare the size of any cluster to this null distribution, thereby identifying the relative alpha level and producing a P value. This non-parametric permutation

approach has a number of advantages relative to more traditional approaches to significance testing with electrophysiological data: Firstly, it makes no a priori assumptions about when or where effects are likely to be apparent; secondly, this approach accounts for multiple comparisons over space and time, which can result in an uncontrolled false positive rate if uncorrected (Kilner, 2013). To summarise: the result of this GLM analysis is that it identifies areas within the candidate networks whose inclusion positively or negatively covaries with individual differences in our behavioural factors, and that these results are fully corrected for multiple comparisons at a whole-brain level.

3. Results

3.1. Behavioural results

The PCA identified three factors, with eigenvalues greater than 0.9, which explained the 76.86% of the total variance. The factor loadings are shown in table 1.

STM assessment

	Factors		
	Order Factor	**Visuo-Spatial STM Factor**	**Visual STM Factor**
Forward Digit Span task	**0.879**	0.184	0.013
Forward Letter Span task	**0.919**	0.181	-0.030
Acoustic Forward Digit Span task	**0.855**	0.142	0.052
Spatial Span task	**0.675**	0.210	-0.114
Visual Pattern task	0.196	**0.804**	-0.141
Visual Change Detection (colour dots)	0.204	**0.835**	0.059
Visual Change Detection (arrows)	-0.025	-0.057	**0.989**

Table 1. Factor loadings scores from PCA of STM assessment. The values in bold are taken in consideration for the interpretation.

The first factor was strongly associated with four tests (Digit, Corsi, Letter and Spoken digit tasks), in these tasks the subject has to remember the given sequence of presentation of an array, independently from the nature of the material to be encoded.

The second factor was associated with the Colour dot and the Visual Pattern task, that is, with visuo-spatial STM. The third factor was associated with just one test, the Direction arrow task, which represents a task of visual STM without any spatial information. We used the factors produced by this analysis to assign a score to each factor for each participant, which will be used in the MEG analysis GLM.

3.2. Meg Results

3.2.1. Temporal ICA

We identified 25 ICs in the beta frequency band. Through the estimate of cross-correlation, we were able to detect those networks that showed the highest degree of spatial correspondence to an independent set of fMRI networks. The beta-band showed high correlation values, thus a good average spatial overlap with fMRI networks (beta-cross-correlation$_{avg}$ = 0.45). As shown in Figure 1 we were able to find the seven MEG RSNs, in the figure it is possible to see also their fMRI counterparts (top panel).

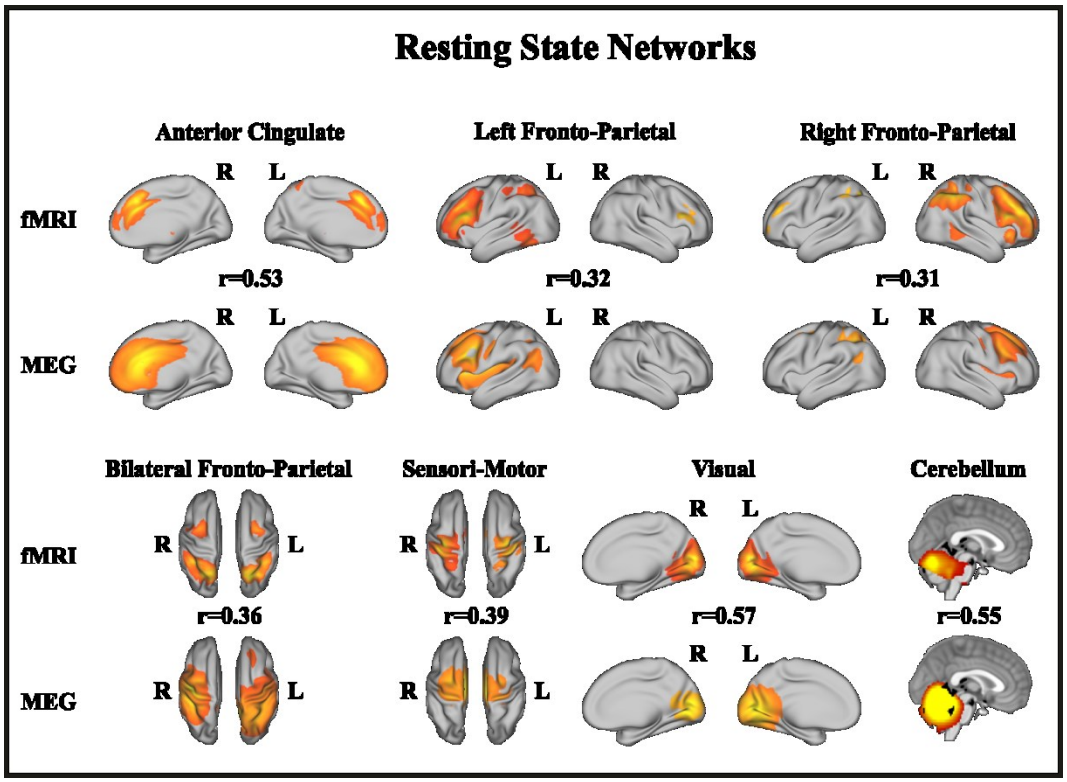

Figure 1. Spatial maps of our MEG RSNs, derived by using the temporal ICA (bottom) and the associated spatial map of fMRI RSNs (Smith et al., 2012) (top). For each network we calculated he cross-correlation values between the two maps (r-values). The threshold for MEG maps is at 2.1 except for left and right fronto-parietal networks that is it at 1.9 and for cerebellum is 3. The threshold of fMRI maps is at 5.

The cross correlation values for each network are shown in Table 2. It is noteworthy that the spatial resolution between the two techniques is different. This difference is noticeable in the bilateral fronto-parietal network, where some areas/nodes in the MEG network are merged compared with the fMRI. These results are in line with previous MEG works (Mantini et al., 2007; Brookes et al., 2011; Barnes et al., 2015).

Cross-Correlation Values

	Beta Band
ACC	0.53
rFPN	0.31
lFPN	0.32
Bilateral FPN	0.36
Sensori-motor Network	0.39
Visual Network	0.57
Cerebellum network	0.55

Table 2. Cross-correlation values between MEG and fMRI networks for seven networks in each frequency band.

3.2.2. Meg-adapted dual regression/GLM

In order to verify our second research hypothesis, namely the possibility that the differences in resting functional connectivity in the fronto-parietal networks could mirror inter-subject differences in STM capacity, we ran a GLM on these networks using the three factors derived from our behavioural PCA analysis. To do this we had to create a whole-brain map for each participant, in which the degree of connectivity with the networks of interest is expressed. We found that connectivity between the left fronto-parietal network and a lower-sensory processing area in temporo-occipital cortex was significantly related to the subject variability in the STM assessment measured outside the scanner.

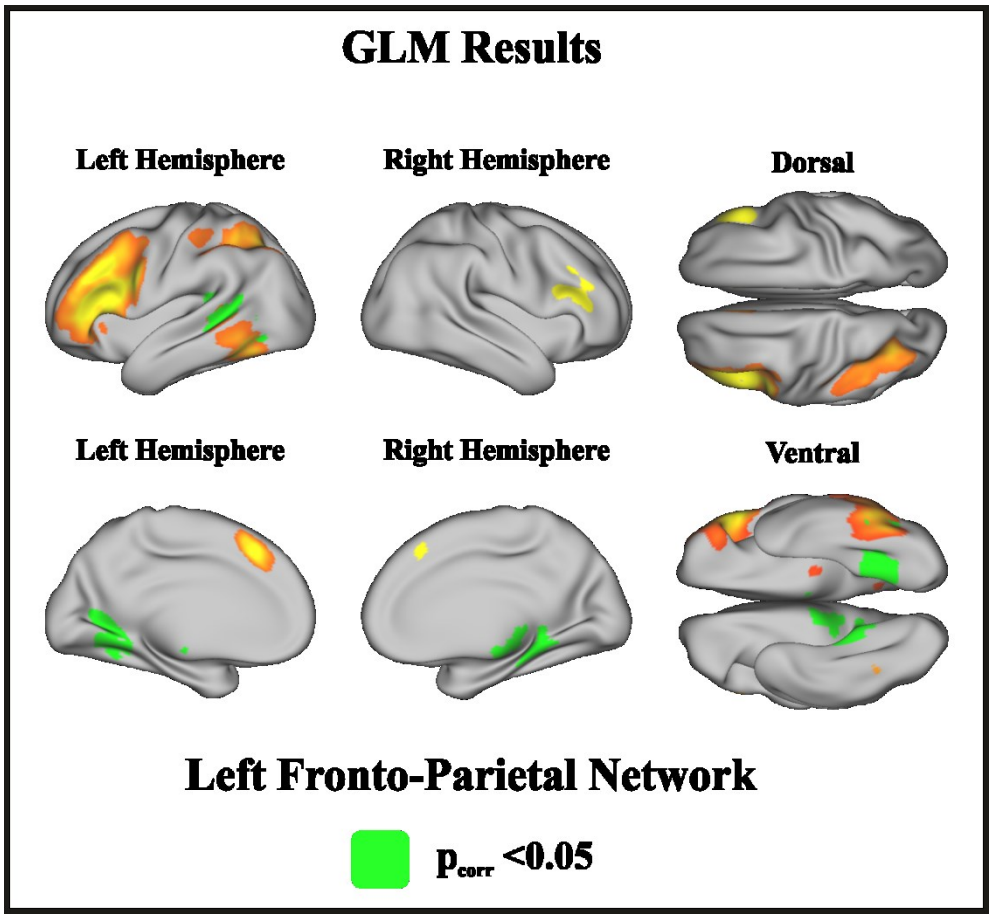

Figure 2. The results of GLM procedure. The green area shows an area of the left fronto-parietal network that correlated significantly with visuo-spatial STM (p_{corr} <0.05)

The behavioural factor that showed the significant correlation with our RSN was the second factor, the visuo-spatial STM. Moreover, this effect survived the permutation cluster correction for multiple comparison (p_{corr} = 0.003). Figure 2 shows this effect with the green regions representing the significant cluster. The cluster was formed by 31 voxels, which span from the temporal to the occipital lobe with the involvement of the bilateral inferior temporal cortex, left and right middle temporal gyrus and left superior temporal gyrus. In order to assess the nature of the relationship between connectivity and STM capacity we calculated the correlation between the strength of connectivity in that area and the visuo-spatial STM factor.

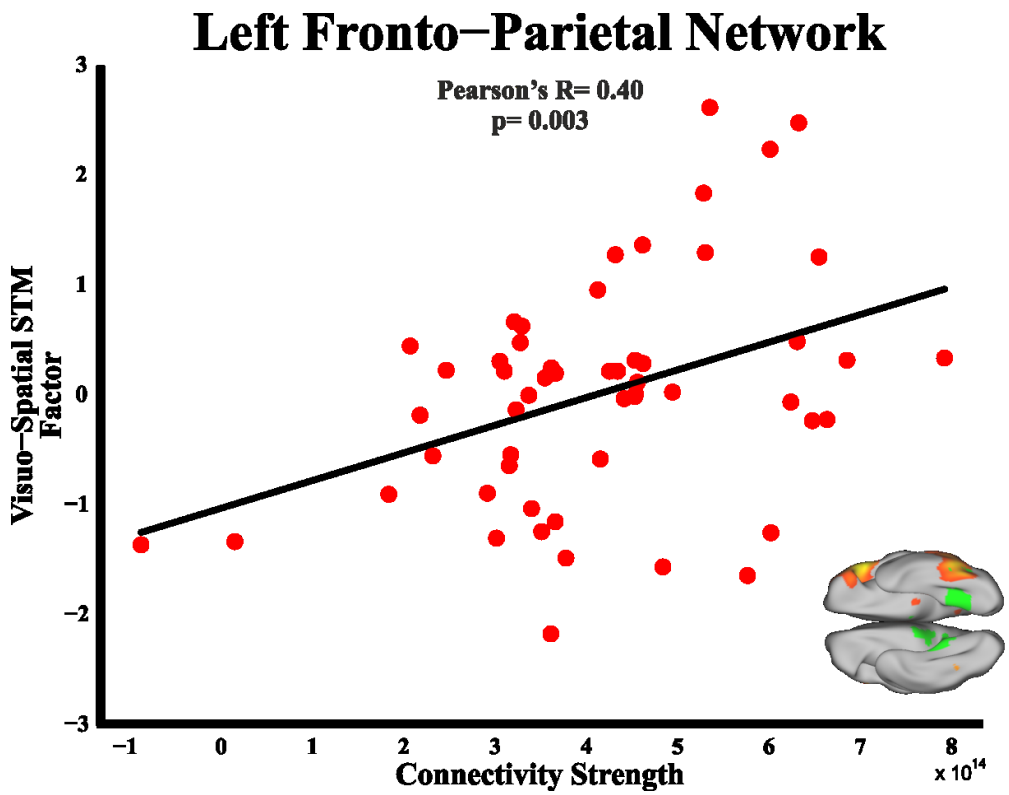

Figure 3. Scatter plot of the relationship between connectivity in the significant area and visuo-spatial STM scores (Pearson's R=0.40). The black solid line represents the regression line.

As a result of this analysis we found a significant positive Pearson correlation (Pearson's r=0.40, p=0.003).This result is shown in Figure 3. To check if our significant correlation was affected by the presence of outliers we calculated Cook's distance, which identifies points that negatively affect the regression model. It also shows the influence of each observation on the fitted response values. The threshold value used for spotting highly influential points was 1. All Cook's distance values measured were smaller than 0.11, and that means that the relationship between connectivity and STM scores were not influenced by single cases.
No other effect survived our multiple comparison correction.

4. Discussion

In this study, the first goal was to demonstrate the feasibility and validity of MEG as a tool to explore resting state functional connectivity. In order to do that we used the

temporal information from the neural oscillation in the beta band to parcellate the brain into separate brain networks. These networks were spatially similar to the ones widely reported in fMRI studies. It is well known that it is possible to obtain RSNs by the direct measure of the dynamic pattern of activity across different brain regions through the use of invasive electrodes recording (see Engel et al., 2001 for a review). The issue with this direct approach is ethical: it is possible to pursue it just from non-human primates or from patients who need brain surgical interventions. Alternatively, the method used in the present study allowed investigating the neural activity of the brain at rest both spatially and temporally with non-invasive recording. We used a particular blind source-separation procedure, the temporal ICA, which allowed us to decompose brain oscillations into distinct independent components. What is remarkable is that this procedure does not require any spatial information because the spatial distribution of our RSNs emerges from the temporal patterns of electrophysiological activity. Therefore, our method is substantially assumption-free and does not depend upon a choice of a particular brain area. With this methodology, we were effectively able to derive RSNs and were also able to use a beamformer source reconstruction to identify seven different networks in our resting state data: ACC network, left, right, and bilateral hemisphere fronto-parietal networks, sensori-motor network, visual network, and cerebellum network. These networks were significantly similar to other RSNs previously observed in an independent fMRI study.

The second goal of this study was to prove that the MEG networks variability is related to STM capacity. Individual differences in STM ability have been investigated by means of psychological research for decades. Here we have demonstrated that the basis of these differences relies on the variability of ongoing brain activity. Our hypothesis was that the functional organization of multiple brain areas involved in multiple cognitive functions could predicts STM capacity in terms of inter-subject variability. We combined MEG data with fMRI spatial set to improve our spatial resolution. The employment of this methodology allowed us to identify the fronto-

parietal networks and then to use the temporal structure of the MEG brain oscillations in these networks to investigate their variable coordination with other brain areas, and finally to use this electrophysiological coordination to prove that it covaries with STM. The use of a spatial set helps to mitigate a common problem in performing connectivity analyses on electrophysiological data. However, our analysis depends upon the temporally downsampled Hilbert envelopes of our MEG recordings. Moreover, the use of this procedure has a great advantage for interpreting differences between subjects in term of networks. Here, we have found that electrophysiological coordination between left fronto-parietal network and a lower-level sensory processing area (temporal cortex) covaried with our subjects' visual-spatial STM capacity. Because our subjects were at rest and not involved in an active task, differences in strategy or motivation cannot account for the relationship between behavioural and connectivity measures. This is one of the greatest advantages to use a resting state paradigm. Moreover, because MEG is a direct measure of neural activity these differences cannot be attributed to basic differences in the vascular system, like using the BOLD response.

The fact that the fronto-parietal network is connected with the temporal lobe might explain the important role that this network plays in controlling an efficient perceptual processing of the material to be encoded. In particular, other studies found the involvement of temporal lobe, and specifically the inferior temporal cortex, in STM or in WM tasks, involving visuo-spatial material (for a review see Logothetis and Sheinberg, 1996). Recent works have stressed the importance of prefrontal cortex for WM and STM, in reactivating the appropriate neural representations in posterior lower-level areas (Ranganath and D'Esposito, 2005; Woloszyn and Sheinberg, 2009). Furthermore, the involvement of the left fronto-parietal network, that includes the middle frontal gyrus, with the frontal eye field (FEF) and the superior parietal cortex, explains the relation with covert and overt spatial attention process (Schwartz et al., 2005; Taylor et al., 2007). Intra-cranial recordings in non-human primates have demonstrated that it is possible to find a neural signature of WM in the sustained cell

responses in the inferior temporal cortex (Chelazzi et al. 1998) and a recent study has proved that when the monkey was involved in an attentional task the FEF signals were mirrored also in visual areas including V4 and inferior temporal cortex (Gregoriou et al., 2009). Our results confirm the merit of MEG recordings for investigating spontaneous brain activity and demonstrated that intrinsic connectivity between fronto-parietal network and lower-level sensory areas can predict visuo-spatial STM.

It is also important to highlight that we could not find any significant correlation with verbal STM. This could be due to different reasons. One could be that subjects use different strategies to retain the verbal material. There are two main mechanisms for storing verbal information: articulatory rehearsal and attentional refreshing. The former is based on language processes while the latter is based on reactivation of memory traces (for a recent review see Camos 2015). The use of different strategies across participants could increase the variability and so create difficulties in finding an unique relationship between connectivity at rest and verbal STM, and this might explain why no difference survives after our conservative correction for multiple comparison. Another reason could rely upon the fact that we chose three networks a priori, based upon their involvement in attention and control mechanisms, but it is possible that they do not comprise all the mechanisms and cortical areas involved in language processing. A final possibility is that MEG is not able to detect the several areas recruited by language processing.

In conclusion, we have demonstrated the importance to use MEG as tool to investigate intrinsic connectivity and that the functional connection between fronto-parietal network and temporal lobe at rest represents an important pathway for successful cognitive performance in STM tasks.

Chapter 4

Does Cognitive Training Enhance Intrinsic Brain Connectivity? A MEG study

1. Introduction

In Chapter 3 we have pointed out the importance of short-term memory (STM) for creating a neural representation of the external world. The brain processes, *stores* and acts on the incoming information. However, representations of the external world are constantly changing, and therefore the brain needs to update these representations constantly. We have also demonstrated that the intrinsic brain activity is the neuronal substrate on which STM capacity relies, and it is well known that resting state connectivity is highly consistent across subjects. Moreover, electrophysiological and neuroimaging techniques indicate that the resting state networks (RSNs) are for a large part predetermined. In the light of these considerations, the aim of the work described in this chapter is to investigate how functional connectivity changes in response to the environment and in particular if it is possible to modify it as a result of cognitive training. This is important not only to understand how the brain codifies its response to change in the external world but also to understand how cognitive rehabilitation can improve mental performance in brain-damaged patients.

In the literature, it has been already demonstrated that, despite predetermination, the RSNs pattern specifically changes after intensive perceptual, motor, or higher function training (Lewis et al., 2009; Voss et al., 2010; Jolles et al., 2013). In particular, there is evidence that the practice of cognitive training changes RSNs, especially the fronto-parietal networks (Olesen et al., 2004; Dahlin et al., 2008; Jolles et al. 2013; Astle et al., 2015). The main goal of our project is to investigate if the RSN connectivity related to STM (for further details see Chapter 3) changes after a STM training. It has been demonstrated that STM plays a fundamental role in executive functions, such as Working Memory (WM), but also in other higher functions such as perceptual awareness (Soto & Silvanto, 2014) and that

improvements in STM extend beyond the specific training tasks (Jaeggi et al., 2008). Therefore, a further aim is to assess if the improvement in STM capacity remains confined to the domain trained or if it is extended also to other domains as a general improvement in encoding and storing perceptual information. In order to do this we recorded 9 minutes of resting state MEG scan and carried out a complete STM assessment before and after STM training. To assess the possibility that the training can affect STM ability in general, regardless of the domain trained, we used three different kinds of training: Verbal, Spatial, or Visual STM.

To summarize our hypothesis: In this study we have attempted to answer the following important questions (a) Does the specificity of training (verbal, spatial or visual) affect the relationship between fronto-parietal networks and the related lower-level domain-specific sensory areas? In addition, (b) Can training enhance the global strength of functional connectivity in the RSNs typically associated with higher-order executive functions?

2. Methods

2.1. Participants

The participants were the same as in the previous study (see Chapter 3). The final dataset comprises data from 54 participants, (mean age = 24.09 years, SD= 4.43, 34 females). They were randomly assigned to one of four conditions: Verbal Group (14 subjects), Spatial Group (16 subjects), Visual Group (14 subjects) and Control Group (10 subjects). Three groups out of four performed one of the three different STM trainings (Verbal, Spatial, Visual) while the fourth group was a control group that did not follow any training. All subjects had normal or corrected-to-normal vision and no history of psychiatric or neurological conditions. All participants gave written informed consent to the participation in the study, which was approved by the University of Cambridge Psychology Research Ethics Committee.

2.2. Cognitive assessment

The same multiple different STM assessments described in Chapter 3 were administered using a tablet computer before and after the training. There were no differences between the groups in the pre-training assessment scores (Verbal STM: $F_{(1,3)}$ =0.333, p=0.802; Spatial STM: $F_{(1,3)}$ =1.524, p=0.220; Visual STM: $F_{(1,3)}$ =0.935, p=0.431). Both pre-training and post-training assessments were conducted by a member of the staff who was blinded to the group where the subjects were allocated.

2.3. Cognitive training

The training groups performed the training at home: it consisted of two training sessions per day that could be done in separate sessions or back-to-back, each session taking no more than 30 minutes (as the subjects improved sessions would take longer since the sequences would get longer). There were 20 training sessions in total spread over 14 days. Subjects were asked to not take more than two days off consecutively. So they trained for 10 out of 14 days. The research team could remotely monitor online the progress of each participant. The training task consisted of one task of the assessment: the Verbal group performed the digit task, the Spatial group performed the similar to Corsi block task, and the Visual group performed the colour visual change detection task; while the control group did not perform any training. All subjects repeated resting state MEG recording and post-training STM assessment within seven days of completing the training.

2.4. Behavioural analysis

For the purpose of analysing the behavioural performance of our subjects, we averaged the three Verbal STM tasks measures, the two Spatial STM tasks measures, and the two Visual STM tasks measures. These composite scores of Verbal, Spatial, and Visual STM were later used to assess the training improvements. In order to establish the effect of the training on participants' STM capacity we carried out a 3-

way Mixed ANOVA using as between factor the group membership (4 levels) and as within factor session time (pre-training and post-training) and STM domains (Verbal, Spatial and Visual)

2.5. MEG data acquisition

We used the same procedure to acquire MEG resting state before and after the training (see Chapter 3).

2.6. MEG analysis

We used the same analysis pipeline of Astle et al. 2015.

2.6.1. Pre-processing, Source Reconstruction, Envelope, and Concatenation

The first stages of the procedure were identical to the one used in the pre-training resting state analysis (see Chapter 3) with the exception of the fact that, in order to assess the connectivity changes after the training, we included both single-subject pre-training and post-training downsampled envelope estimates. This leads to the creation of a single dataset including the data of all the subjects temporally concatenated.

2.6.2. MEG-adapted dual regression

At this stage, we used again the MEG-adapted dual regression procedure as in the Chapter 3 on the same three networks in the beta band: the left, the right fronto-parietal networks, and the bilateral fronto-parietal network. As a result of this procedure, we obtained for each participant a whole-brain map, which corresponds to voxel-by-voxel electrophysiological connectivity with each of our three networks before and after the training procedure.

2.6.3. Group level regression analysis (GLM)

As last step we tested whether our candidate RSNs or the interconnections with other areas were affected as a result of training. In particular, we wanted to verify if there

was a general improvement of STM capacity independently from the domain trained and/or if we could find changes in connectivity associated with the trained domain. In order to test our hypothesis we used four different whole-brain GLM procedures. To explore the association between changes in intrinsic connectivity and STM capacity we conducted a GLM containing the information regarding the impact of the training regardless of the group membership. In this way, we ran the GLM in which the first regressor corresponded to the relationship between STM scores and connectivity after the training (in this case measured as average of the three composite scores), and the second regressor corresponded to the relationship between STM scores and connectivity before the training. We repeated this procedure for Verbal, Spatial and Visual scores with other three GLM procedure. These GLMs allowed us to explore the relationship between intrinsic connectivity and STM ability after the training while controlling for any relationship before the training. In other words, we tested for an association between changes in STM capacity and changes in functional connectivity. We also added a regressor, which corresponded to the subject mean for each participant.

Then, we adopted the same procedure used in Chapter 3 to correct for multiple comparisons.

3. Results

3.1. Behavioural Results

The ANOVA showed that the main effect of both session time and STM were significant, $F(1,50) = 22.68$, $p = 0.0001$, $p\eta^2 = 0.31$ and $F(2,100) = 4.58$, $p = 0.013$, $p\eta^2 = 0.08$, respectively. Moreover, we found a significant interaction between group and STM domain, $F(6,100) = 7.15$, $p = 0.0001$, $p\eta^2 = 0.30$. A Bonferroni post-hoc correction revealed a significant difference in the Visual STM training group, with higher scores than the Verbal and Spatial STM domains (both p-values = 0.001), see figure 1.

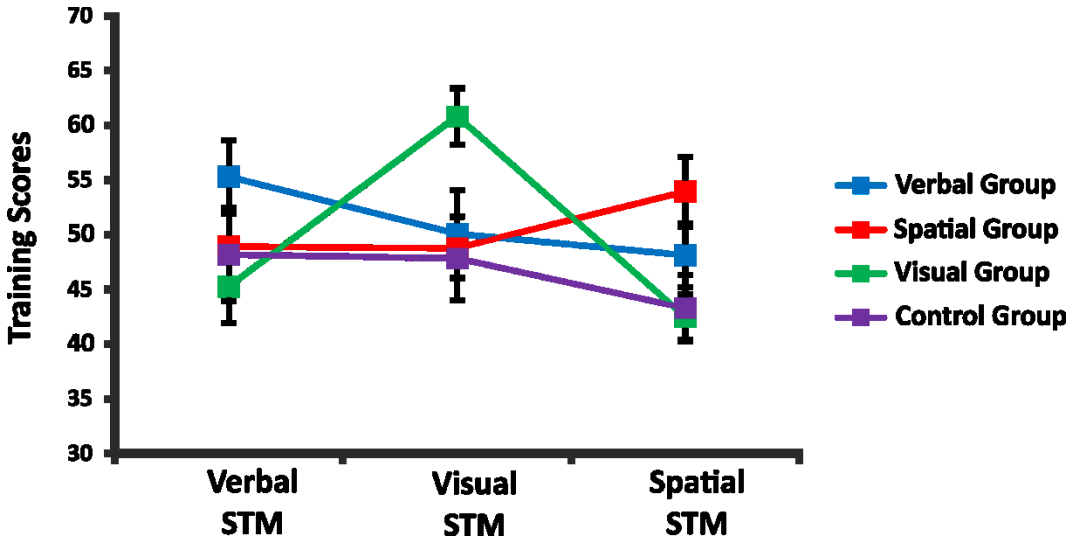

Figure. 1 Significant Interaction between Group Membership and STM domain. Bonferroni corrected post hoc analysis of the subjects in the different domains of STM as a function of group membership.

We found also another significant interaction among group membership STM domain and time session, $F(6,100) = 3.61$, $p = 0.003$, $p\eta^2 = 0.18$.

	Verbal STM scores Pre vs Post	**Spatial STM scores Pre vs Post**	**Visual STM scores Pre vs Post**
Verbal Group	**p= 0.001**	**p=0.020**	p=0.482
Spatial Group	**p=0.003**	**p=0.001**	p=0.717
Visual Group	p=0.056	p=0.218	**p=0.024**
Control Group	p=0.670	p=0.104	p=0.787

Table. 1 - Bonferroni corrected p-value in the post hoc of the subjects in the different domains of STM before and after training as a function of group membership.

This interaction can be explained by the Bonferroni corrected post-hoc testing that showed that for the Verbal Group there was an improvement after the training in both Verbal and Spatial STM domain ($p = 0.001$ and $p= 0.02$ respectively); the same

improvement was found in both domains in the Spatial Group (Verbal STM p = 0.003, Spatial STM p = 0.001); finally the visual group showed a significant improvement just in Visual STM domain (p = 0.024). In contrast this was not the case for the control group (all p-value >0.05), see table 1 and figure 2.

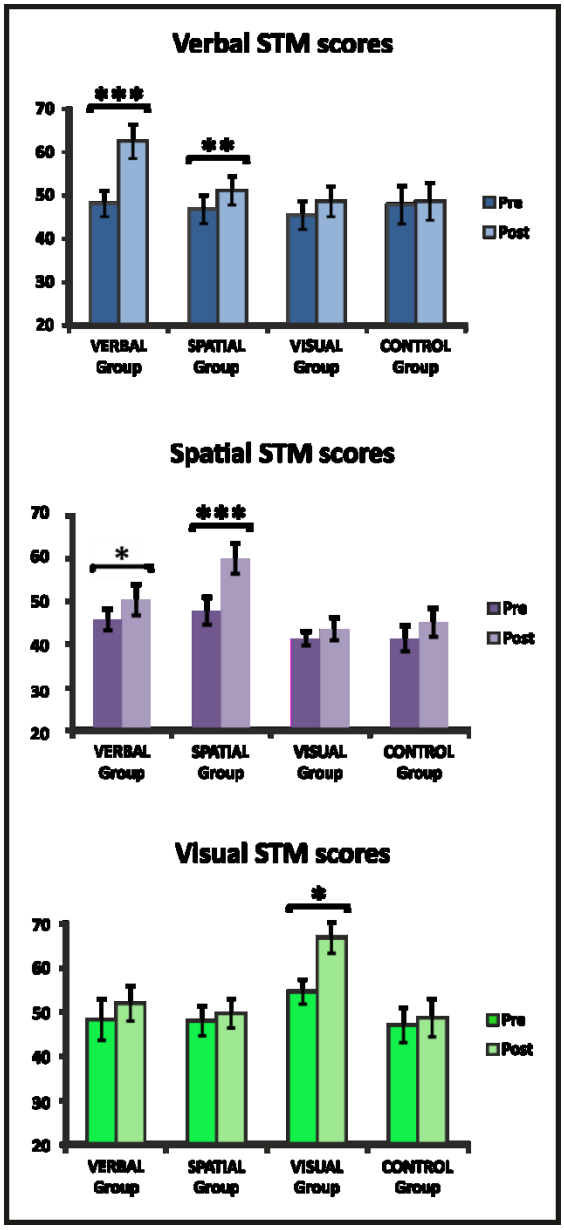

Figure 2. Significant interaction among time session, STM domain and Group membership. Behavioural scores of the subjects in the different domains of STM before and after training as a function of group membership. The stars indicate the Bonferroni corrected p-value in the post hoc (* p<0.05; ** p<0.005; *** p<0.001 comparisons).

3.2. MEG Results

In order to verify our second hypothesis, namely the possibility that training could modify the resting state functional connectivity in the fronto-parietal networks, we ran four different GLMs on these networks using as regressor the behavioural scores before and after the STM training. To do that we created a whole-brain map for each participant in which the degree of connectivity with the networks of interest was expressed. As a result, no effect survived to our multiple comparison correction.

4. Discussion

In the present study, we examined if STM training can enhance STM capacity and if such effect would be mirrored by changes in resting brain connectivity. Moreover, we wanted to assess if the effect of training in just one domain could be generalized and yield a general improvement in STM. To do that we recorded resting state activity before and after STM training in four different subject groups. In three groups subjects performed one of the three different STM trainings (Verbal, Spatial, and Visual) while the fourth group was a control group that did not follow any training.

We found that after 20 sessions of STM training STM ability was substantially increased especially in the domain in which subjects were trained as demonstrated by two significant interactions (see Figure 1 and 2). This effect was not present in the Control group. What is remarkable is that both the Spatial and Verbal Group improved in both Spatial and Verbal STM domains while the Visual Group improved just in the Visual STM domain. This pattern can be explained by the nature of the training tasks: in both Spatial and Verbal training, the subject has to memorize the order in which the items are presented while in the Visual training task the subject has only to detect the presence or absence of a change of an item in the array. This can explain the significant interaction between STM domain and Group membership

(Figure 1). The fact that in the Verbal and Spatial tasks the subjects must encode and retain the order of presentation of certain quantity of items might promote the use of a similar encoding strategy. It has been demonstrated that training improvements are related to the choice of a successful strategy (for a recent review see Klingberg, 2010). Indeed, our training might have improved or changed the subjects' strategy resulting in a greater efficacy in memorizing a set of items (locations or digits). Perhaps performance improvements are related to the use of chunking strategy: an ability to reorganize materials into familiar or structured sequences (Ericcson et al., 1980). The use of chunking is not efficient for a visual detection task, which, instead, promotes the use of visual search strategies. This can explain why Spatial and Verbal group improved in both Spatial and Verbal STM while Visual group improved just in Visual STM.

All that said, the substantial improvements of behavioural performance were not mirrored by changes in subjects' functional connectivity. There are several possible explanations for this. First, despite that the 20 sessions of training were sufficient to increase the STM capacity at behavioural level more sessions might be needed to change intrinsic brain connectivity. Second, each group had done a different kind of training that might promote a different kind of strategy and this could create an increment of variability in neurocognitive processes. For example Bor and colleagues (2003) found that the use of structured chunks as encoding strategy correlated with the activation of the lateral frontal cortex, the inferior parietal lobule and the fusiform gyrus while during unstructured sequence (i.e. requiring the use of visual strategy to encode the sequences) they found a recruitment of bilateral parietal and premotor areas. Therefore, the use of different strategies may make more complicated to identify significant relationships with RSNs, especially when applying a conservative correction for multiple comparisons. Third, we investigated only the beta band and it could be that the neural processing underlying training affects other frequency bands. Moreover, we chose seed networks that have a consistent role in control-demanding tasks (Lepsien et al., 2005), but it is possible that training affects interconnections

with other sensory-specialized areas (Smith et al., 1996). A final related possibility is that functional connectivity changes in resting state networks are less detectable using MEG than other neuroimaging techniques.

5. Future Direction

In the present study, we used MEG resting state to investigate changes in functional connectivity after STM training. We could not identify any significant relationship between changes in performance and changes in connectivity. In future experiments, it would be interesting to try new approaches. First of all, it could be worth looking at different frequency bands in the oscillatory activity. Second, because it is possible that training might affect lower-level sensory areas we could focus on sensory networks. Third, because different training domains created a great variability of our data we could implement the GLM to test the improvement linked to the specific training. This means that our analysis should focus on finding a significant interaction between time and group, using a paired t-test on within-subject effects of each group against the control group. Lastly, to avoid the influences of individual strategy based on task demand we could develop a new training procedure that includes all the tasks used here in an unique session. Furthermore, it could be worth including an active control group (i.e. placebo group). This control group should receive a believable alternative training to control for effects of expectancy, a factor that is known to have influence on cognitive performance. To do that, one possibility could be to use in the placebo group a similar training program as the active group with the difference that it does not become progressively more difficult depending on participant's performance.

- **References**

- Ajina S., Bridge H. (2016) Blindsight and Unconscious Vision: What They Teach Us about the Human Visual System. Neuroscientist. Oct 23. pii: 1073858416673817
- Ajina, S., Kennard, C., Rees, G., Bridge, H. (2015). Motion area V5/MT+ response to global motion in the absence of V1 resembles early visual cortex. Brain. 138(Pt 1):164-78. doi: 10.1093/brain/awu328.
- Astle, D.E., Barnes, J.J., Baker, K., Colclough, G.L., Woolrich, M.W. (2015). Cognitive training enhances intrinsic brain connectivity in child-hood. J Neurosci 2015; 35: 6277-6283.
- Awh, E., Jonides, J. (2001). Overlapping mechanisms of attention and spatial working memory. Trends Cogn Sci. 5(3):119–126.
- Azzopardi, P., and Cowey, A. (2001). Motion discrimination in cortically blind patients. Brain. 124, 30–46.
- Bagattini, C., Mazzi, C., and Savazzi, S. (2015). Waves of awareness for occipital and parietal phosphines perception. Neuropsychologia 70, 114–125. doi:10.1016/j.neuropsychologia.2015.02.021
- Barbur, J. L., Watson, J. D., Frackowiak, R. S., & Zeki, S. (1993). Conscious visual perception without V1. Brain, 116(Pt 6), 1293–1302.
- Barnes, J.J, Woolrich, M.W., Baker, K., Colclough, G.L., Astle, D.E. (2015). Electrophysiological measures of resting state functional connectivity and their relationship with working memory capacity in childhood. Dev Sci. Advance online publication. doi:10.1111/desc.12297.
- Beckmann, C. F., Mackay, C. E., Filippini, N., and Smith, S. M. (2009). Group comparison of resting-state FMRI data using multi-subject ICA and dual regression. Neuroimage 47(Suppl. 1), S148.
- Bell, A.J., and Sejnowski, T.J. (1995). An information-maximization approach to blind separation and blind deconvolution. Neural Comput. 7, pp. 1129–1159
- Benjamini, Y., and Yekutieli, D. (2001). The control of the false discovery rate in multiple testing under dependency. Annals of Statistics 29, 1165–1188.
- Berman, R.A., and Wurtz, R.H. (2010). Functional identification of a pulvinar path from superior colliculus to cortical area MT. J Neurosci 30: 6342–6354.
- Bollini, A., Sanchez-Lopez, J., Savazzi, S., Marzi, C.A. Lights from the dark: Neural responses from a blind visual hemifield. Frontiers in Neuroscience, submitted.

- Bor, D., Duncan, J., Wiseman, R.J. & Owen, A.M. (2003). Encoding strategies dissociate prefrontal activity from working memory demand. Neuron, 37, 361±367.
- Brainard, D. H. (1997). The psychophysics toolbox. Spatial Vision, 10, 433–436.
- Brignani, D., Guzzon, D., Marzi, C.A., & Miniussi, C. (2009). Attentional orienting induced by arrows and eye-gaze compared with an endogenous cue. Neuropsychologia, 47, 370–381.
- Brookes, M.J., Woolrich, M., Luckhoo, H., Price, D., Hale, J.R., Stephenson, M.C., Barnes, G.R., Smith, S.M., Morris, P.G. (2011). Investigating the electrophysiological basis of resting state networks using magnetoencephalography.Proc Natl Acad Sci U S A 108:16783–16788.
- Brookes, M.J., Woolrich, M.W., Barnes, G.R. (2012). Measuring functional connectivity in MEG: a multivariate approach insensitive to linear source leakage. Neuroimage. 63:910–920.
- Buchner, H., Gobbele, R., Wagner, M., Fuchs, M., Waberski, T.D., Beckmann, R. (1997). Fast visual evoked potential input into human area V5. Neuroreport 8: 2419–2422.
- Camos, V. (2015). Storing verbal information in working memory. Current Directions in Psychological Science, 24, 440–445.
- Celeghin, A., Savazzi, S., Barabas, M., Bendini, M., Marzi, C.A. (2015a). Blindsight is sensitive to stimulus numerosity and configuration: evidence from the redundant signal effect. Exp Brain Res. 233(5):1617-23.
- Celeghin, A., Barabas, M., Mancini, F., Bendini, M., Pedrotti, E., Prior, M., Cantagallo, A., Savazzi, S., Marzi, C.A. (2015b). Speeded manual responses to unseen visual stimuli in hemianopic patients: what kind of blindsight? Conscious Cogn. 32:6-14
- Chelazzi, L., Duncan, J., Miller, E.K., Desimone, R. (1998). Responses of neurons in inferior temporal cortex during memory-guided visual search. Journal of Neurophysiology 80:2918–2940.
- Coch, D., Skendzel, W., Grossi, G., & Neville, H. (2005). Motion and color processing in school-age children and adults: an ERP study. Developmental Science, 8, 372–386.
- Corsi, P. M. (1972). "Human memory and the medial temporal region of the brain". Dissertation Abstracts International. 34 (2): 891.
- Cowey, A. (2010). The blindsight saga. Exp Brain Res. 200(1):3-24. doi: 10.1007/s00221-009-1914-2.
- Crawford, J. R., and Garthwaite, P.H. (2005). Testing for suspected impairments and dissociations in single-case studies in neuropsychology: Evaluation of

alternatives using Monte Carlo simulations and revised tests for dissociations". Neuropsychology, 19, 318-331.

- Crick, F. (1995). The Astonishing Hypothesis: The Scientific Search for the Soul (Reprint ed.). Scribner.
- Crick, F., & Koch, C. (1998). Consciousness and Neuroscience. Cerebral Cortex, 8, 97–107.
- Cowan, N., Elliott, E. M., Saults, J. S., Morey, C. C., Mattox, S., Hismjatullina, A. (2005). On the capacity of attention: Its estimation and its role in working memory and cognitive aptitudes. Cognitive Psychology, 51, 42-100.
- Dehaene, S., and Naccache, L. (2001). Towards a cognitive neuroscience of consciousness: Basic evidence and a workspace framework. Cognition. 79, 1–37.
- Dahlin, E., Neely, A.S., Larsson, A., Backman L., Nyberg, L. (2008). Transfer of learning after updating training mediated by the striatum. Science 320:1510–1512.
- Deco, G., Corbetta, M. (2011). The dynamical balance of the brain at rest Neuroscientist, 17, pp. 107–123
- Della Sala, S., Gray, C., Baddeley, A., & Wilson, L. (1997). The Visual Patterns Test: A new test of short-term visual recall. Feltham, Sufolk: Thames Valley Test Company.
- Delorme, A., and Makeig, S. (2004). EEGLAB: an open source toolbox for analysis of single-trial EEG dynamics including independent component analysis. J Neurosci Methods. 134(1):9-21.
- de Pasquale, F., Della Penna, S., Snyder, A.Z., Lewis, C., Mantini, D., Marzetti, L, Belardinelli, P., Ciancetta, L., Pizzella, V., Romani, G.L., Corbetta, M. (2010). Temporal dynamics of spontaneous MEG activity in brain networks. Proc Natl Acad Sci. 107:6040–6045.
- Desimone, R, Duncan, J. (1995). Neural mechanisms of selective visual attention. Annu Rev Neurosci. 18:193–222.
- De Vries, M., Van Dijk, B., Spekreijse, H. (1989). Motion onset-offset VEPs in children. Electroenceph Clin Neurophysiol 74: 81–87.
- Di Lollo, V., Enns, J. T., and Rensink, R. A. (2000). Competition for consciousness among visual events: The psychophysics of reentrant visual processes. Journal of Experimental Psychology: General, 129, 481–507.
- Efron, B., and Tibshirani, R.J. (1993). An Introduction to the Bootstrap. Chapman Hall, New York, NY
- Engel, A.K., Fries, P., Singer, W. (2001). Dynamic predictions: Oscillations and synchrony in top-down processing. Nat Rev Neurosci 2: 704–716.
- Engle, R.W., Kane, M.J., Tuholski, S.W. (1999). Individual differences in working memory capacity and what they tell us about controlled attention,

general fluid intelligence, and functions of the prefrontal cortex. Models of working memory: Mechanisms of active maintenance and executive control. Cambridge University Press, Editors: Miyake, Akira and Shah, Priti, pp.102-134.

- Ericcson, K.A., Chase, W.G., and Falloon, S. (1980). Acquisition of a memory skill. Science 208, 1181–1182.
- Ffytche, D.H., Guy, C.N., Zeki, S. (1995). The parallel visual motion inputs into areas V1 and V5 of human cerebral cortex. Brain 118: 1375–1394.
- Ffytche, D. H., Guy, C. N., Zeki, S. (1996). Motion specific responses from a blind hemifield. Brain. 119(Pt 6), 1971–1982.
- Ffytche, D.H., and Zeki, S. (2011). The primary visual cortex, and feedback to it, are not necessary for conscious vision. Brain. 134(Pt 1):247-57. doi: 10.1093/brain/awq305.
- Filippini, N., MacIntosh, B.J., Hough, M.G., Goodwin, G.M., Frisoni, G.B., et al. (2009). Distinct patterns of brain activity in young carriers of the APOE-epsilon4 allele. Proceedings of the National Academy of Sciences, USA, 106 (17), 7209–7214. doi:10.1073/pnas.0811879106
- Friston, K. (2002), Beyond phrenology: what can neuroimaging tell us about distributed circuitry? Annu Rev Neurosci.; 25:221–50.
- Friston, K.J. et al., (1994). Statistical parametric maps in functional imaging: A general linear approach. Human Brain Mapping, 2(4), pp.189–210. http://doi.wiley.com/10.1002/hbm.460020402.
- Friston, K. (2008). Hierarchical models in the brain. PLoS Computational Biology 4(11): e1000211.
- Fuchs, M., Wagner, M., Kastner, J. (2001). Boundary element method volume conductor models for EEG source reconstruction. Clin Neurophysiol. 112, 1400-1407.
- Fukuda, K., Vogel, E., Mayr, U., Awh, E. (2010). Quantity, not quality: the relationship between fluid intelligence and working memory capacity. Psychon Bull Rev 17: 673–679.
- Galletti, C., Gamberini, M., Kutz, D.F. (2001). The cortical connections of area V6: an occipito-parietal network processing visual information. Eur J Neurosci 13:1572–1588.
- Gazzaley, A, Nobre, A.C. (2012). Top-down modulation: bridging selective attention and working memory. Trends Cogn Sci.16 (2):129–135.
- Gregoriou, G.G., Gotts, S.J., Zhou, H., & Desimone, R. (2009). High-frequency, long-range coupling between prefrontal and visual cortex during attention. Science, 324 (5931), 1207–1210. doi:10.1126/science.1171402

- Gross, C.G. (1991). Contribution of striate cortex and the superior colliculus to visual function in area MT, the superior temporal polysensory area and the inferior temporal cortex. Neuropsychologia 29: 497–515.
- Hipp, J.F., Hawellek, D.J., Corbetta, M., Siegel, M., Engel, A.K. (2012). Large-scale cortical correlation structure of spontaneous oscillatory activity. Nat Neurosci. 15:884–890.
- Jaeggi S.M., Buschkuehl M., Jonides J., Perrig W.J. A (2008). Improving fluid intelligence with training on working memory. Proc Natl Acad Sci U S 105(19):6829–33. doi:10.1073/pnas.0801268105.
- Jeffreys, D.A., and Axford, J.G. (1972). Source locations of pattern-specific components of human visual evoked potentials. I. Component of striate cortical origin. Exp. Brain Res. 16:1–21.
- Jolles, D.D., van Buchem, M.A., Crone, E.A., Rombouts S.A. (2013). Functional brain connectivity at rest changes after working memory training. Hum. Brain Mapp.;34:396–406.
- Kaernbach C., Schröger E., Jacobsen T., Roeber U. (1999). Effects of consciousness on human brain waves following binocular rivalry. Neuroreport. 10, 713-716.
- Kavcic, V., Triplett, R.L., Das, A., Martin, T., Huxlin,K.R. (2015). Role of inter-hemispheric transfer in generating visual evoked potentials in V1-damaged brain hemispheres. Neuropsychologia. 68:82-93. doi: 10.1016/j.neuropsychologia.2015.01.003.
- Kenemans, J.L., Kok, A., Smulders, F.T. (1993) Event-related potentials to conjunctions of spatial frequency and orientation as a function of stimulus parameters and response requirements. Electroencephalogr Clin Neurophysiol. 88, 51-63.
- Kilner, J.M. (2013). Bias in a common EEG and MEG statistical analysis and how to avoid it. Clin Neurophysiol 124, 2062–2063.
- Klingberg, T. (2010). Training and plasticity of working memory.Trends in Cognitive Sciences, 14(7), 317–324. doi:10.1016/j.tics.2010.05.002
- Koivisto, M., and Grassini, S. (2016). Neural processing around 200 ms after stimulus-onset correlates with subjective visual awareness. Neuropsychologia84:235-43. doi: 10.1016/j.neuropsychologia.2016.02.024.
- Koivisto, M., and Rientamo, E. (2016). Unconscious vision spots the animal but not the dog: Masked priming of natural scenes. Conscious Cogn. 41:10-23
- Koivisto, M., Salminen-Vaparantam,N., Grassini, S., Revonsuo, A. (2016). Subjective visual awareness emerges prior to P3. Eur J Neurosci. 43(12):1601-11. doi: 10.1111/ejn.13264.

- Lamme, V. (2010). How neuroscience will change our view on consciousness. Cognit. Neurosci.1, 204–240. doi: 10.1080/17588928.2010.497585.
- Lamme, V. A., and Roelfsema, P. R. (2000). The distinct modes of vision offered by feedforward and recurrent processing. Trends in Cognitive Neurosciences, 23, 571–579
- Lee, C., Miyakoshi, M., Delorme, A., Cauwenberghs, G., Makeig, S. (2015). Non-parametric group-level statistics for source-resolved ERP analysis. Conf Proc IEEE Eng Med Biol Soc. 2015:7450-3. doi: 10.1109/EMBC.2015.7320114.
- Lee, T.W., Girolami, M., Sejnowski, T.J.(1999). Independent component analysis using an extended infomax algorithm for mixed subgaussian and supergaussian sources. Neural Comput. 11(2):417-41.
- Lepsien, J., Griffin, I.C., Devlin, J.T., & Nobre, A.C. (2005). Directing spatial attention in mental representations: Interactions between attentional orienting and working-memory load. NeuroImage, 26 (3), 733–743. doi:10.1016/j.neuroimage.2005.02.026
- Lewis, C.M., Baldassarre, A., Committeri, G., Romani, G.L., Corbetta, M. (2009). Learning sculpts the spontaneous activity of the resting human brain. Proc Natl Acad Sci U S A 106:17558–17563.
- Linden, D.E.J. (2005). The P300: where in the brain is it produced and what does it tell us? Neuroscientist. 11:563–76. doi: 10.1177/1073858405280524.
- Logothetis, N.K., and Sheinberg, D.L. (1996) Visual object recognition. Annual review of neuroscience; 19:577–621.
- Luck, S.J., & Vogel, E.K. (1997). The capacity of visual working memory for features and conjunctions. Nature, 390, 279–281.
- Luckhoo, H. (2014). Investigating the role of APOE-a4, a risk gene for Alzheimer's disease, on functional brain networks using magnetoencephalography. PhD dissertation, University of Oxford.
- Luckhoo, H.T., Brooke,s M.J., Woolrich, M.W. (2014). Multi-session statistics on beamformed MEG data. Neuroimage 95:330 –335.
- Luckhoo,H., Hale, J.R., Stokes, M.G., Nobre, A.C., Morris, P.G., Brookes, M.J., Woolrich, M.W. (2012). Inferring task-related networks using independent component analysis in magnetoencephalography. Neuroimage 62:530–541.
- Makeig, S., Bell, A.J., Jung, T.P., Sejnowski, T.J. (1996). Independent component analysis of electroencephalographic data. Adv. Neural Inf. Process. Syst. 8, pp. 145–151
- Makeig, S., Westerfield, M., Townsend, J., Jung, T.P., Courchesne, E., Sejnowski, T.J. (1999). Functionally independent components of early event-related potentials in a visual spatial attention task. Philos Trans R Soc Lond B Biol Sci. 354, 1135-1144.

- Mayer, J.S., Bittner, R.A., Nikolic, D., Bledowski, C., Goebel, R., Linden, D.E. (2007). Common neural substrates for visual working memory and attention. Neuroimage. 36(2):441–453.
- Mangun, G.R. (1995). Neural mechanisms of visual selective attention. Psychophysiology.32, 4-18.
- Mantini, D., Perucci, M.G., Del Gratta, C., Romani, G.L., Corbetta, M. (2007). Electrophysiological signatures of resting state networks in the human brain. Proc. Natl Acad. Sci. USA 104, 13170–13175.
- Martens, S., Munneke, J., Smid, H., Johnson, A. (2006). Quick minds don't blink: electrophysiological correlates of individual differences in attentional selection. J Cogn Neurosci. 18, 1423-1438.
- Marzi, C.A., Bisiacchi, P., Nicoletti, R. (1991). Is interhemispheric transfer of visuomotor information asymmetric? Evidence from a meta-analysis. Neuropsychologia. 34(2):1163–1177.
- Mazzi, C., Bagattini, C., Savazzi, S. (2016). Blind-Sight vs. Degraded-Sight: Different Measures Tell a Different Story. Front Psychol. 7:901. doi: 10.3389/fpsyg.2016.00901.
- Mazzi, C., Mancini, F., Savazzi, S. (2014). Can IPS reach visual awareness without V1? Evidence from TMS in healthy subjects and hemianopic patients. Neuropsychologia. 64,134–144. doi: 10.1016/j.neuropsychologia.2014.09.026.
- Milner, A.D. (1998). Insights into blindsight. Trends Cogn Sci. 1; 2(7):237-8. doi: 10.1016/S1364-6613(98)01185-1.
- Olesen, P.J., Westerberg, H., Klingberg, T. (2004). Increased prefrontal and parietal activity after training of working memory. Nat. Neurosci 7:75–79.
- Panagiotaropoulos, T., Kapoor, V., Logothetis, N.K. (2014). Subjective visual perception: from local processing to emergent phenomena of brain activity. Philos Trans R Soc Lond B Biol Sci. 369(1641):20130534.
- Pascual-Marqui, R.D., Esslen, M., Kochi, K., Lehmann, D. (2002). Functional mapping of electric neuronal activity with zero localization error: standardized low resolution brain electromagnetic tomography (sLORETA). NeuroImage Vol. 16, No. 2.
- Pitzalis, S., Strappini, F., De Gasperis, M., Bultrini, A., and Di Russo, F. (2012). Spatio-temporal brain mapping of motion-onset VEPs combined with fMRI and retinotopic maps. PLoS ONE 7:e35771. doi: 10.1371/journal.pone.0035771.
- Poeppel, E., Held, R., & Frost, D. (1973). Residual visual function after brain wounds involving the central visual pathways in man. Nature, 243 (5405), 295–296.
- Potts, G.F., Tucker, D.M. (2001). Frontal evaluation and posterior representation in target detection. Brain Res Cogn Brain Res. 11, 147-56.

- Potts, G.F., Liotti, M., Tucker, D.M., Posner, M.I. (1996). Frontal and inferior temporal cortical activity in visual target detection: Evidence from high spatially sampled event-related potentials. Brain Topography.9:3–14.
- Ranganath, C., D'Esposito, M. (2005). Directing the mind's eye: prefrontal, inferior and medial temporal mechanisms for visual working memory. Current opinion in neurobiology; 15:175–182.
- Riddoch, G. (1917). Dissociation of visual perceptions due to occipital injuries, with especial reference to appreciation of movement. Brain; 40: 15–57
- Schenk, T., Zihl, J. (1997). Visual motion perception after braindamage: I. Deficits in global motion perception. Neuropsychologia;35:1289–97
- Rutman, A.M., Clapp, W.C., Chadick, J.Z., Gazzaley, A. (2010). Early topdown control of visual processing predicts working memory performance. J Cogn Neurosci. 22(6):1224–1234.
- Schwartz, S., Vuilleumier, P., Hutton, C., Maravita, A., Dolan,R.J., Driver, J. (2005). Attentional load and sensory competition in human vision: modulation of fMRI responses by load at fixation during task-irrelevant stimulation in the peripheral visual field. Cerebral Cortex, 15 (6), 770–786. doi:10.1093/cercor/bhh178
- Schmid, M. C., and Maier, A. (2015). To see or not to see – Thalamo-cortical networks during blindsight and perceptual suppression. Progress in Neurobiology, 126, 36-48. doi: 10.1016/j.pneurobio.2015.01.001.
- Schmid, M.C., Mrowka, S.W., Turchi, J., Saunders, R.C., Wilke, M., Peters, A.J., Ye, F. Q., and Leopold, D. A. (2010). Blindsight depends on the lateral geniculate nucleus. Nature; 466: 373–7.
- Schmolesky, M.T., Wang, Y., Hanes, D.P., Thompson, K.G., Leutgeb, S., Schall, J.D., Leventhal, A.G. (1998). Signal timing across the macaque visual system. J Neurophysiol 79: 3272–3278.
- Schoenfeld, M.A., Heinze, H.J., Woldorff, M.G. (2002). Unmasking motion-processing activity in human brain area V5/MT mediated by pathways that bypass primary visual cortex. Neuroimage 17: 769–779.
- Sergent, C., Baillet, S., Dehaene, S. (2005). Timing of the brain events underlying access to consciousness during the attentional blink. Nat Neurosci. 8 (10):1391-400.
- Shafto, J.P., Pitts, M.A. (2015). Neural Signatures of Conscious Face Perception in an Inattentional Blindness Paradigm. J Neurosci. 5; 35(31):10940-8.
- Shefrin, S.L., Goodin, D.S., Aminoff, M.J. (1988). Visual evoked potentials in the investigation of "blindsight". Neurology. 38(1):104-9.
- Sincich, L.C., Park, K.F., Wohlgemuth, M.J., Horton, J.C. (2004). Bypassing V1: a direct geniculate input to area MT. Nat Neurosci 7: 1123–1128.

- Sligte, I.G., Scholte, H.S., Lamme, V.A.F. (2008). Are There Multiple Visual Short-Term Memory Stores? PLoS ONE, 3(2), e1699.
- Smith, E.E., Jonides, J., & Koeppe, R.A. (1996). Dissociating verbal and spatial working memory using PET. Cerebral Cortex, 6 (1), 11–20.
- Smith, S.M., Mille,r K.L., Moeller, S., Xu, J., Auerbach, E.J., Woolrich, M.W., Beckmann, C.F., Jenkinson, M., Andersson, J., Glasser, M.F., Van Essen, D.C., Feinberg, D.A., Yacoub, E.S., Ugurbil, K. (2012). Temporally-independent functional modes of spontaneous brain activity. Proc Natl Acad Sci U S A109:3131–3136.
- Smith, S.M., Miller, K.L., Moeller, S., Xu, J., Auerbach, E.J., Woolric,h M.W., Beckmann, C.F., Jenkinson, M., Andersson, J., Glasser, M.F., Van Essen, D.C., Feinberg, D.A., Yacoub, E.S., Ugurbil, K. (2012). Temporally-independent functional modes of spontaneous brain activity. Proc Natl Acad Sci U S A109:3131–3136.
- Soto D., Silvanto J., (2014) Reappraising the relationship between working memory and conscious awareness. Trends Cogn. Sci., 18, pp. 520–525.
- Stevens, A.A., Tappon, S.C., Garg, A., & Fair, D.A. (2012).Functional brain network modularity captures inter- and intra-individual variation in working memory capacity. PLoS ONE, 7 (1), e30468. doi:10.1371/journal.pone.0030468
- Tagliabue, C.F., Mazzi, C., Bagattini, C., Savazzi, S. (2016). Early Local Activity in Temporal Areas Reflects Graded Content of Visual Perception. Front Psychol. 7:572. doi: 10.3389/fpsyg.2016.00572.
- Tamietto, M., Morrone, M.C. (2016). Visual plasticity: blindsight bridges anatomy and function in the visual system. Current Biology; 26(2):R70–R73.
- Taylor, P.C., Nobre, A.C., Rushworth, M.F. (2007). FEF TMS affects visual cortical activity. Cerebral Cortex, 17 (2), 391–399. doi:10.1093/cercor/bhj156
- Tong, F. (2003). Primary visual cortex and visual awareness. Nature Reviews Neuroscience, 4, 219–229.
- van Dam, W. O., Decker, S. L., Durbin, J. S., Vendemia, J. M. C. & Desai, R. H. (2015). Resting state signatures of domain and demand-specific working memory performance. Neuroimage, 118, 174–182. doi:10.1016/j.neuroimage.2015.05.017
- Van Veen, B.D., van Drongelen, W., Yuchtman, M., Suzuki, A. (1997). Localization of brain electrical activity via linearly constrained minimum variance spatial filtering. IEEE Trans Biomed Eng 44:867– 880. CrossRef Medline
- Voss M.W., Prakash R.S., Erickson K.I., Basak C., Chaddock L., Kim J.S., Alves H., Heo S., Szabo A.N., White S.M., Wo´ jcicki T.R., Mailey E.L., Gothe N., Olson E.A., McAuley E., Kramer A.F. (2010). Plasticity of brain networks in a randomized intervention trial of exercise training in older adults. Front Aging Neurosci 2.

- Weiskrantz, L., Warrington, E. K., Sanders, M. D., & Marshall, J. (1974). Visual capacity in the hemianopic field following a restricted occipital ablation. Brain, 97(4), 709–728.
- Wens, V., Bourguignon, M., Goldman, S., Marty, B., Op de Beeck, M., Clumeck, C., Mary, A., Peigneux, P., Van Bogaert, P, Brookes, M.J.,et al. (2014a). Inter- and intra-subject variability of neuromagnetic resting state networks. Brain Topogr. 27:620–634.
- Wens, V., Mary, A., Bourguignon, M., Goldman, S., Marty, B., Op de Beeck, M., Van Bogaert, P., Peigneux, P., De Tiège, X. (2014b). About the electrophysiological basis of resting state networks.Clin Neurophysiol. 125:1711–1713.
- Woloszyn, L., Sheinberg, D.L. (2009). Neural dynamics in inferior temporal cortex during a visual working memory task. J Neurosci 29:5494–5507.
- Woolrich, M.W., Jbabdi, S., Patenaude, B., Chappell, M., Makni, S., Behrens, T., Beckmann, C, Jenkinson, M., Smith, S.M. (2009). Bayesian analysis of neuroimaging data in FSL. Neuroimage 45:S173–S186.
- Zeki, S., ffytche, D.H. (1998). The Riddoch syndrome: insights into the neurobiology of conscious vision. Brain. 121 (Pt 1):25-45.

- **Acknowledgements**

Here I am, at the end of this thesis after three really intensive years. During this period at the University of Verona, I believe that I have matured as a scientist in what is one of my greatest passions, the Neuroscience world, but more than anything that I matured as a person. I have met many people on this journey, many friends and many mentors. I would like to dedicate these last few lines to those who believed in me, who bore these trying years along with me, and who bore with me.

First and foremost I want to thank my supervisor Carlo Alberto Marzi for freely contributing his time and ideas, and for making my PhD experience productive and stimulating. His great knowledge and his advice on both research, as well as, on being a scientist have been much appreciated.

My thanks also goes to Silvia Savazzi without whose precious support, it would not have been possible to conduct this research.

I would like to also thank Duncan Astle, who, although was not my official supervisor, gave me invaluable advice and gave me the opportunity to join his team at MRC in Cambridge. I really appreciated his help and contribution to this thesis and for infecting me with his enthusiasm for research. I want to also thank all the people at MRC for taking me in and making me feel part of the team. A special and huge thanks is for my officemates Chiara and Gina for listening to me, putting up with me, and sharing both good and bad times. I thank my labmates and all the other people who I have met along the way for the stimulating discussions and for all the fun we have had in the last three years over lots of cookies.

Last but not least, I would like to thank my family for all of the sacrifices made on my behalf and for supporting me throughout this PhD.

I would like that these acknowledgements mark an end point but also a starting point because I believe that we never stop growing, and I hope to reach new goals and to tackle new challenges.

Grazie a tutti!